

# Late Mesoproterozoic to earliest Neoproterozoic basin record of the Sibao orogenesis in western South China and relationship to the assembly of Rodinia

Matthew R. Greentree<sup>a,\*</sup>, Zheng-Xiang Li<sup>a</sup>, Xian-Hua Li<sup>b</sup>, Huaichun Wu<sup>c</sup>

<sup>a</sup> *Tectonics Special Research Centre, School of Earth and Geographical Sciences,  
The University of Western Australia, Crawley, WA 6009, Australia*

<sup>b</sup> *Key Laboratory of Isotope Geochronology and Geochemistry, Guangzhou Institute of Geochemistry,  
Chinese Academy of Sciences, Guangzhou 510640, China*

<sup>c</sup> *State Key Laboratory of Geological Processes and Mineral Resources, China University of Geosciences, Beijing 100083, China*

Received 18 October 2005; received in revised form 19 July 2006; accepted 11 August 2006

## Abstract

New geochronological and geochemical constraints on the 5000–9000 m thick Precambrian sedimentary and volcanic successions exposed along the western margin of the South China Block indicate the presence of two distinct tectonostratigraphic successions. The earliest, termed here the Laowushan Formation, comprises of volcanic rocks such as alkali basalts, breccias and tuff that are atypical of the sedimentary rocks in the previously defined Kunyang Group. A tuff within the Laowushan Formation yielded a SHRIMP U–Pb zircon age of  $1142 \pm 16$  Ma. The alkali basalts have a geochemical signature similar to basalts found in modern intracontinental rifts, with a uniform Nd isotopic character ( $\epsilon_{\text{Nd}} = -0.87$  to  $+0.84$ ). New U–Pb geochronology constrains the depositional age of the Kunyang Group to between ca. 1000 and 960 Ma, contemporaneous with the peak of the Sibao Orogeny. The succession largely consists of siltstone, sandstone and limestone deposited in marine, lagoonal and fluvial environments. Detrital zircon ages record changes in provenance from dominantly Archean (ca. 3570–2660 Ma) and Paleoproterozoic (ca. 1950–1800 Ma) ages in the basal and middle parts of the succession to predominately Paleoproterozoic (2140–1730 Ma) and smaller Mesoproterozoic to earliest Neoproterozoic (ca. 1500–1200 and 1093–960 Ma) components at the top of the succession. We interpret the Laowushan Formation and the Kunyang Group to be deposited during separate basin-forming events. The earliest, at ca. 1140 Ma, is interpreted to be an intracontinental rift basin, but the presence of exotic detrital grains may indicate a local early collision between the Yangtze and Cathaysia Blocks prior to the Sibao Orogeny. We suggest a tectonic scenario similar to the modern Rhine Graben where extension occurs orthogonally to the orogenic front. The traditionally defined Kunyang Group represents a foreland basin sequence which received increasingly juvenile sediments from an uplifted Sibao orogenic belt during the late Mesoproterozoic–earliest Neoproterozoic closure of the remaining ocean between the Yangtze and Cathaysia Blocks.

© 2006 Elsevier B.V. All rights reserved.

**Keywords:** Sibao Orogeny; Kunyang Group; Detrital provenance; Yangtze; Mesoproterozoic; Foreland basin; Alkali basalts; Rodinia

## 1. Introduction

The Yangtze and Cathaysia Blocks are believed to have come together to form the South China Block at either ca. 1000 Ma (e.g. Jahn et al., 1990; Li, 1998; Li et al., 2002b) or between 870 and 820 Ma (e.g. Hao et

\* Corresponding author. Tel.: +61 8 6488 7840;  
fax: +61 8 6488 1037.

E-mail address: [mgreentree@tsrc.uwa.edu.au](mailto:mgreentree@tsrc.uwa.edu.au) (M.R. Greentree).

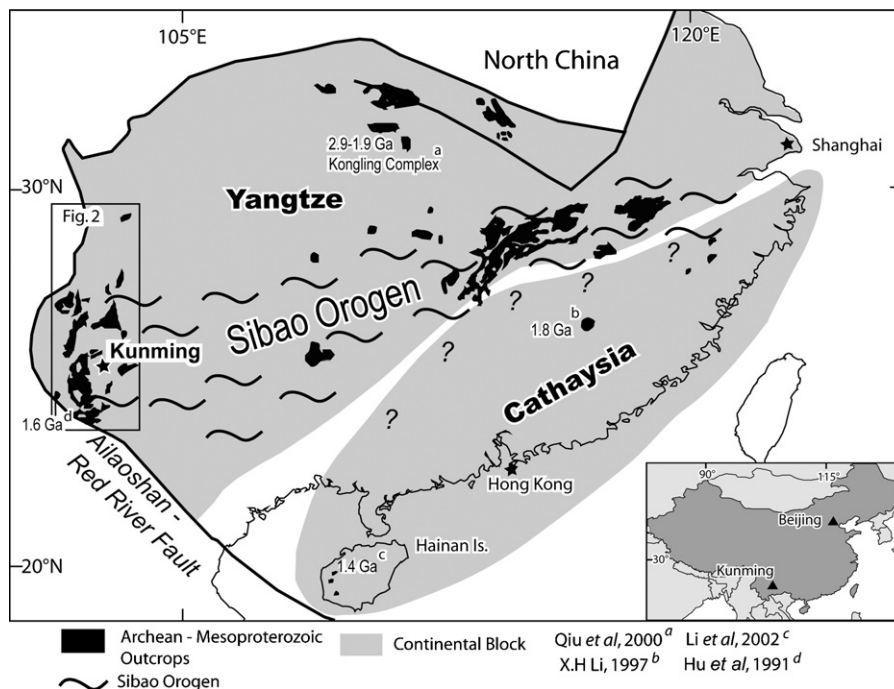


Fig. 1. Tectonic framework of the South China Block and location of outcropping pre-900 Ma rocks (modified after Li et al., 2002b).

al., 1992; Zhao and Cawood, 2000). Widespread deformation, uplift and regional unconformities found across the South China Block are attributed to this collisional orogenesis (e.g. Li, 1998). The term Sibao Orogeny was recommended by Li (1998) to use for describing this orogenic event in place of a variety of terms introduced by local geologists (e.g. the Jinning movement, etc.).

Late Mesoproterozoic to earliest Neoproterozoic rocks on the South China Block consist of sedimentary and rare volcanic rocks. This is in contrast to the mid-Neoproterozoic (ca. 820–750 Ma) rocks found in the region, which typically consist of a large portion of felsic and mafic volcanic rocks (e.g. Li, 1998; Li et al., 2003). The extent and significance of the late Mesoproterozoic to earliest Neoproterozoic sedimentary basins are poorly understood, as is the temporal-spatial evolution of the Sibao Orogeny. Li et al. (2002b) proposed that ca. 1000 Ma quartzites, thought to be equivalent to the Kunyang Group, were deposited in a foreland basin formed along the southern Yangtze Block in response to the Sibao Orogeny. A population of ca. 1400 Ma detrital zircons, thought to have been sourced from the Cathaysia, were found in these quartzites, suggesting that the amalgamation of the two blocks may have begun by ca. 1000 Ma (Li et al., 2002b). This collisional event may represent the closure of oceans between Laurentia–Cathaysia, Yangtze and Australia, thus plac-

ing South China in a central location within Rodinia (Li et al., 1995, 2002b; Li and Powell, 2001).

Successions of late Mesoproterozoic to earliest Neoproterozoic rocks outcrop in western South China along a north–south trending zone (Figs. 1 and 2) traditionally called the “Kangdian Axis” by local geologists (e.g. Ran, 1990; Ruan et al., 1991). In this paper, we present SHRIMP zircon ages of volcanic rocks and detrital zircon ages of clastic rocks, along with geochemical analyses of the rare basaltic rocks, found within the successions. These data provide precise age constraints for the Kunyang Group and enable us to better understand the tectonic evolution of the southern Yangtze Block during the Sibao Orogeny.

## 2. Geological background

The late Mesoproterozoic–earliest Neoproterozoic rocks exposed to the north of the Ailaoshan-Red River Fault include the Kunyang, Huili, Dongchuan and Xide Groups, depending on their geographic locations (Figs. 3 and 4). There is no exposed contact between the Kunyang Group and an older crystalline basement. As a result, various gneissic and high grade metamorphic rocks (e.g. the Kangding complex and Dahongshan Group) in the region had been interpreted as the Paleoproterozoic or Archean basement in the past

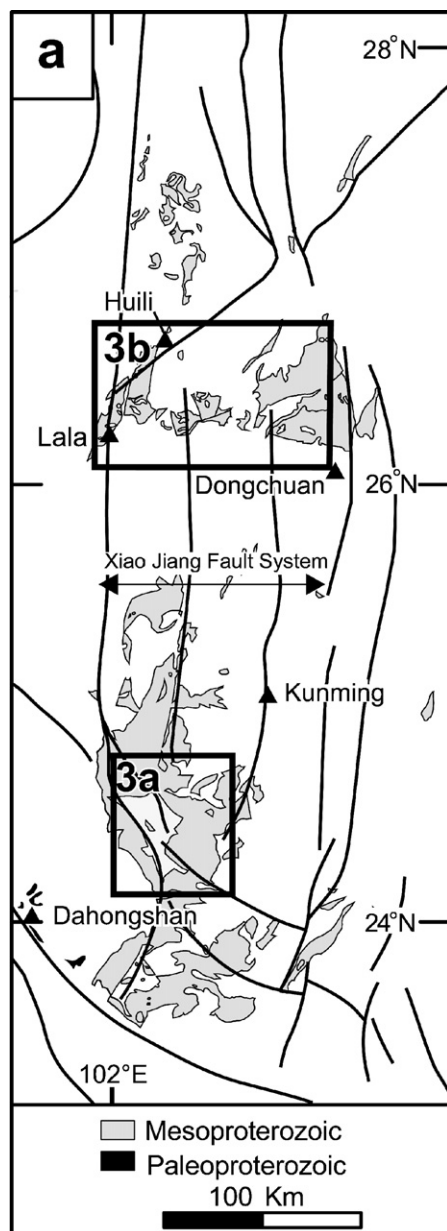


Fig. 2. Outcrop of the Paleoproterozoic–earliest Neoproterozoic rocks along the western margin of the South China Block.

(Yunnan, 1987; Ruan et al., 1991). However, recent precise geochronology indicates that most of these rocks are either Neoproterozoic (ca. 824–764 Ma) in age and are younger than the sub-greenschist facies rocks of the Kunyang Group (Zhou et al., 2002a; Li et al., 2003), or are similar in age to the Kunyang Group (Li et al., 2002b). Nonetheless, the Paleoproterozoic age obtained by Hu et al. (1991) for the upper greenschist–amphibolite facies rocks of the Dahongshan Group has been confirmed by a new SHRIMP zircon age of ca. 1675 Ma (Greentree and

others, unpublished data). Although limited in extent, these rocks are so far the oldest found in the region and the most likely basement rocks for the late Mesoproterozoic sedimentary successions. Upper greenschist facies Hekou Formation in southern Sichuan has been correlated to the Dahongshan Group, but at present no reliable age constraint is available to test this correlation.

Structural trends in this region have a strong Cenozoic overprint. The two major structures in the region are the Ailaoshan–Red River and the Xiao Jiang faults. In Yunnan and Sichuan Provinces, movement along the Cenozoic Xiao Jiang fault system has caused left-lateral block rotation and lateral extrusion towards the southeast (e.g. Burchfiel and Wang, 2003). Within the area termed the Yunnan Block by Burchfiel and Wang (2003), intense Cenozoic deformation is responsible for uplift and block rotations, disrupting the Precambrian rock units and thus making systematic analysis of Precambrian basins more difficult.

### 2.1. Geology of the Kunyang Group

Stratigraphic systems like the Kunyang, Dongchuan, Huili and Xide Groups were based on different type sections, and reflect lateral facies changes and a lack of outcrop continuity between regions. The stratigraphic scheme adopted for the Kunyang Group in this study was from the 1:200,000 Kunming geological map sheet (Kunming, 1971), except that we suggest an additional stratigraphic unit, the Laowushan Formation, for describing the volcanic and sedimentary rocks found in the Yinmin County (Fig. 5). The definition of this unit is based on the results of field mapping, geochronology and geochemical data presented in this paper.

The Kunyang Group is subdivided into nine formations, which from the base up are: the Huangcaoling, Heishantou, Dalongkou, Meidang, Yinmin, Louxue, Eshantou, Luzhijiang and Liubatang Formations (e.g. 1:200,000 geological map sheet; Kunming, 1971). Estimations of the total thickness of the Kunyang Group range between 5000 and 9300 m (e.g. 1:200,000 geological map sheets; Kunming, 1971; Yuxi, 1973). However, structural replications of stratigraphic units that occur in some tightly folded sections may not have been taken into account in these estimates.

Previous geochronological constraints for the Kunyang Group (e.g. Yang et al., 1986; Wu et al., 1990; Chen and Ran, 1992; Ma and Bai, 1998; Zhang et al., 2003) were based on traditional U–Pb and Pb evaporation methods, whole rock Sm–Nd model ages, and Rb–Sr and K–Ar dating. An examination of these data suggests

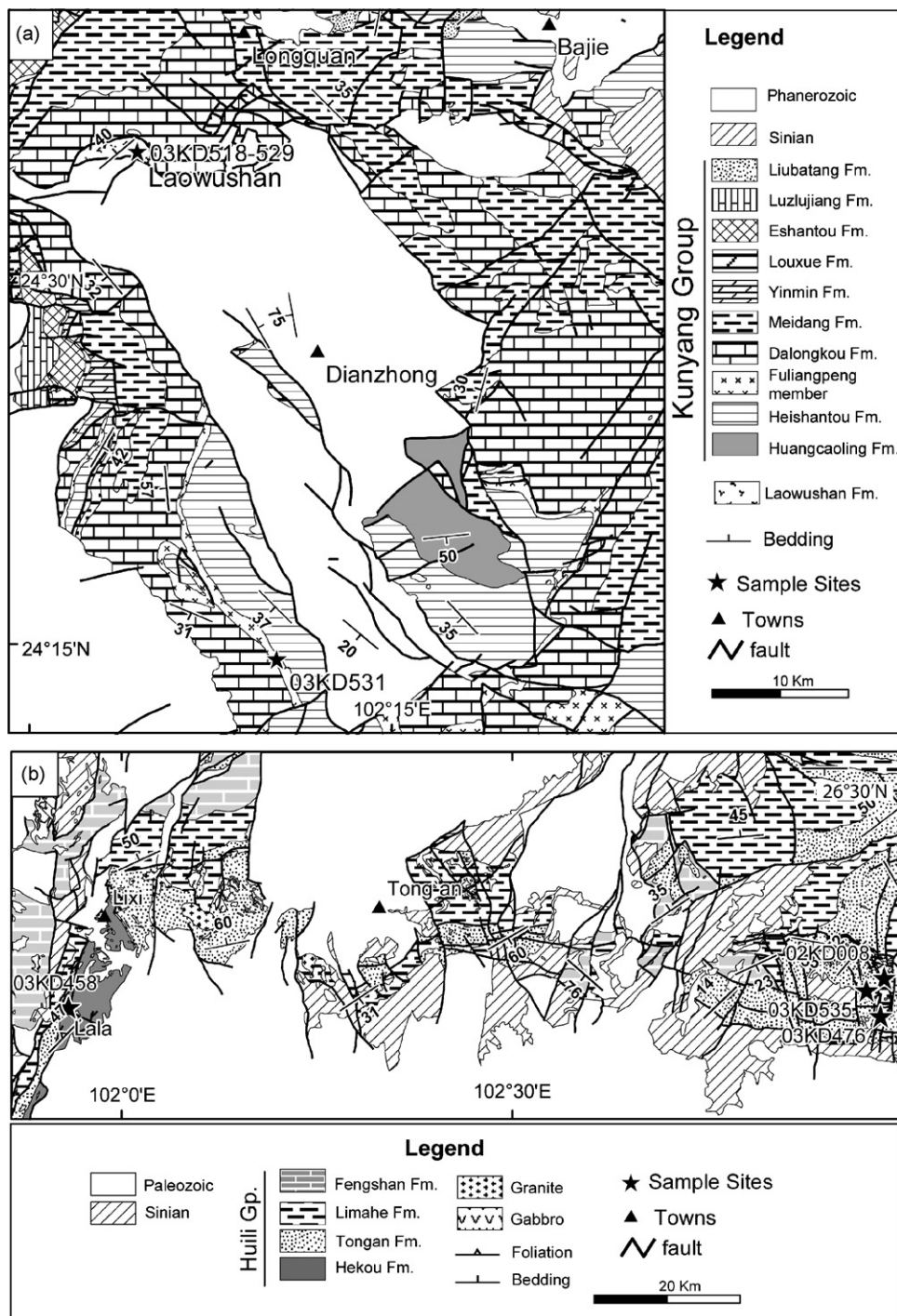


Fig. 3. Simplified geological map of the Mesoproterozoic to earliest Neoproterozoic rocks in western Yangtze. Positions of two study regions are shown in Fig. 2: (a) the Kuyang Group in central Yunnan Province (Kunming, 1971) and (b) the Huili and Dongchuan Groups in southern Sichuan and northern Yunnan Provinces (Yongren, 1965; Huili, 1967).



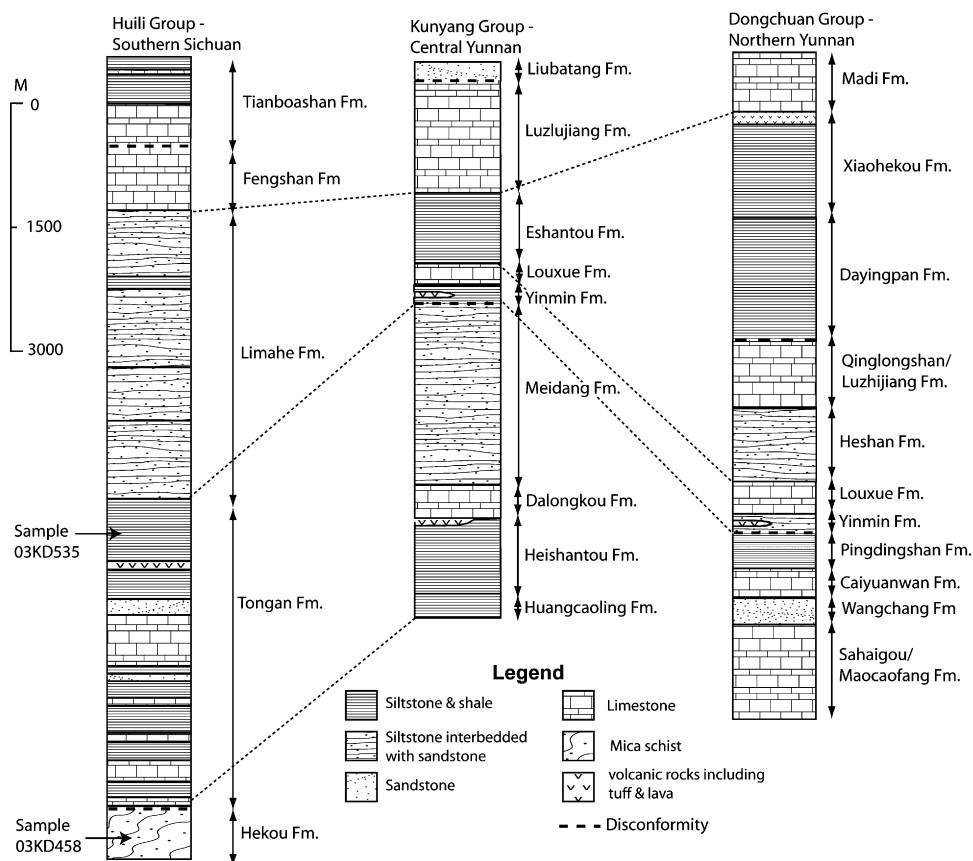


Fig. 4. Comparison and correlation of the different stratigraphic systems used for the late Mesoproterozoic–earliest Neoproterozoic sedimentary successions in the western Yangtze.

that most of the previous Pb–Pb and U–Pb zircon ages are either detrital or inherited zircon ages. Most of the Rb–Sr and K–Ar ages were published without providing data, therefore their qualities cannot be assessed.

The Kunyang Group consists of carbonate-dominated (the Dalongkou, Louxue and Luzhijiang Formations) and siliciclastic-dominated (the Huangcaoling, Meidang, Yinmin, Eshantou and Liubatang Formations) units. Of these units, only two contain rare volcanic rocks such as tuff and basalt (the Yinmin and Heishantou Formations). The Kunyang Group has sedimentary features suggesting progressively shallowing water depth. The basal units (i.e. the Huangcaoling and Heishantou Formations) of the Kunyang Group are composed of sediments indicative of deposition in an anoxic deep water environment. The stratigraphically higher units are either carbonate dominated (i.e. the Dalongkou, Louxue and Luzhijiang Formations) or contain siliclastic sedimentary rocks with structures consistent with deposition in a shallow sea (e.g. the Yinmin Formation) or fluvial environments (e.g. the Liubatang Formation).

The Huangcaoling Formation is the basal unit of the Kunyang Group; it consists largely of black carbonaceous shale. The overlying Heishantou Formation consists mostly of fine-grained grey siltstone, with rhythmic bedding and thin sandstone beds. At the top of this unit is the Fuliangpeng Member, characterised by the presence of several tuffaceous horizons. A unit previously mapped as the Fuliangpeng Member is found in the Yimen County, but it contains a sequence of vesicular basalts, volcanic breccia, tuff and siltstone (Fig. 5). It differs significantly from those described in the type section of the Fuliangpeng Member and has a significantly older age (see Section 4). We thus term these rocks the Laowushan Formation that is distinct from, and underlies, the Kunyang Group (see Sections 4.1 and 6.2). The Dalongkou Formation, which overlies the Heishantou Formation, largely consists of well-bedded carbonate rocks with minor shale and fine-grained sandstone layers.

The Yinmin Formation consists of purple shale and fine-grained sandstone and carbonate. The shale has thinly laminated (<5 mm) bedding and shallow water

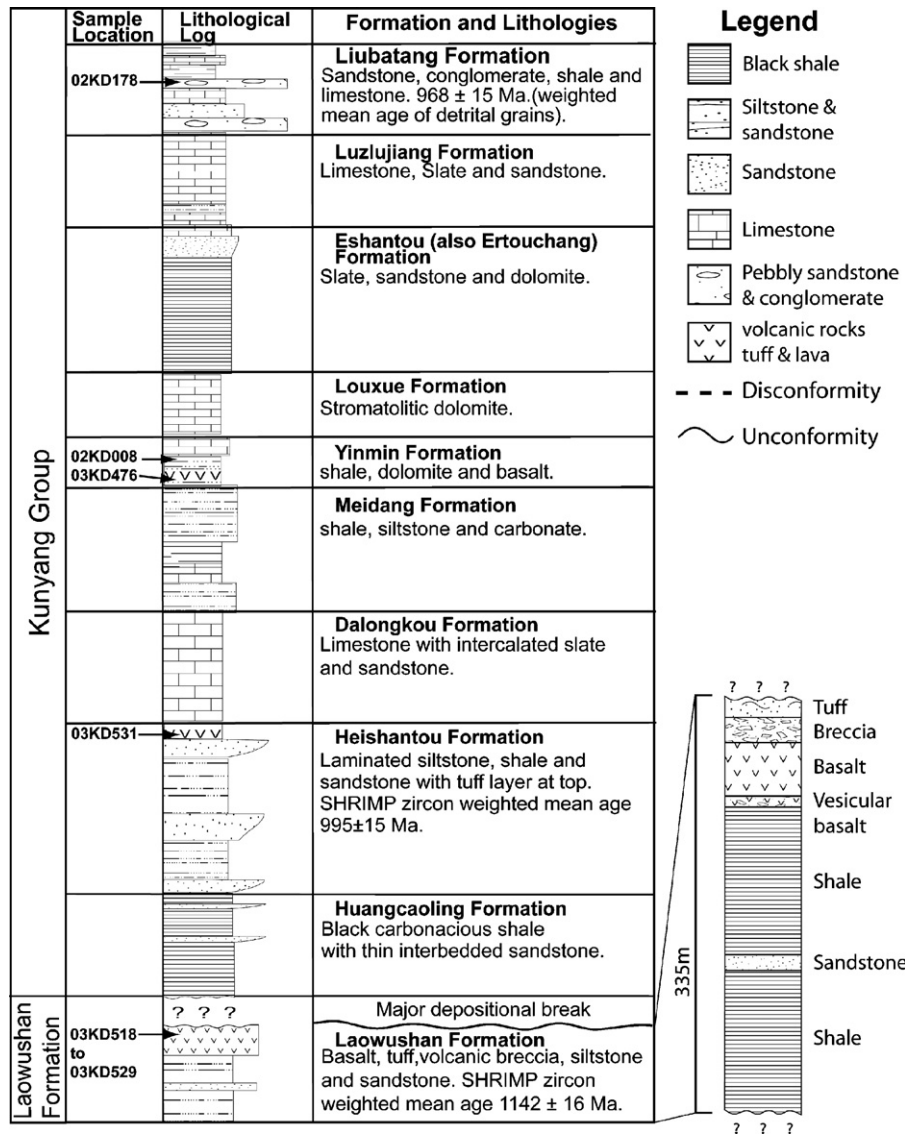


Fig. 5. The stratigraphy of the Kunyang Group as used in this study is derived from the 1:200,000 map (Kunming, 1971) combined with data from field mapping. Radiometric age constraints shown in this figure are all derived from this study. The stratigraphy of the Laowushan Formation is enlarged to show details of this newly defined unit.

sedimentary structures such as ripple marks. Ripple marks found in the Dongchuan area trend  $\sim 200^\circ$ , suggesting a paleo-shore line orientated in an east–west direction. The Yinmin shale has a purple coloured hematite staining, which along with shallow water sedimentary structures, suggests a lacustrine or tidal mud flat in an arid environment (e.g. Ran, 1983, 1989). Evaporitic minerals including gypsum and halite casts have been reported in the Dongchuan area (e.g. Xiong et al., 1995). Numerous breccia bodies found in the Yinmin Formation have been attributed to the migration of halite layers as diapirs (Ruan et al., 1991). The upper layers

of the Yinmin Formation grade into the stromatolitic dolomite of the Louxue Formation, which is interpreted as a lagoonal deposit (e.g. Ran, 1989; Ruan et al., 1991). The dolomites of the Louxue Formation host the strati-form Fe–Cu mineral deposits in this region.

Black carbonaceous shales mark the base of the Eshantou Formation. The presence of these black shales may suggest a return to a more anoxic environment, possibly linked to a period of basin subsidence. However, the overlying Luzhijiang Formation consists of predominately carbonate, suggesting an oxygen-rich marine environment.

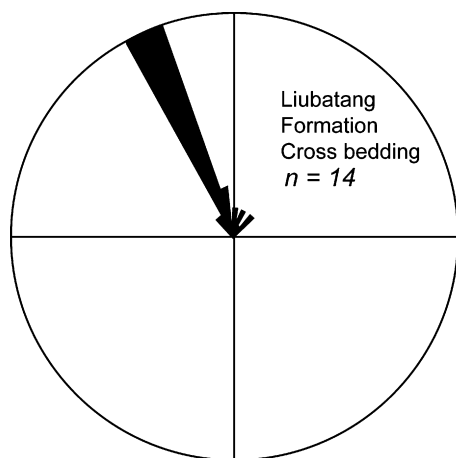


Fig. 6. Paleocurrent directions are measured from the cross-bedded sandstone of the Liubatang Formation.

The Liubatang Formation represents the stratigraphic top of the Kunyang Group and has the most distinctive lithologies. It contains largely siliciclastic rocks including conglomerate, quartz sandstone, shale and some carbonate. The lithological changes and the sedimentary structures suggest a change to fluvial deposition. Paleocurrent directions suggest that sediments were derived from the present-day southeast (Fig. 6).

### 3. Analytical methods

#### 3.1. SHRIMP U–Pb zircon dating

SHRIMP U–Pb dating has been used to determine the age of zircons from tuffs and fine-grained sedimentary rocks (average grain size  $<80\text{ }\mu\text{m}$ ). Zircon concentrates were mounted with zircon standard CZ3 ( $\sim 550\text{ ppm U}$ ,  $^{206}\text{Pb}/^{238}\text{U} = 0.0914$ ; Pidgeon et al., 1994). Both optical photomicrographs and cathodoluminescence images were used for guiding isotopic spot selection. U–Pb isotopic analysis were undertaken using the SHRIMP-II ion microprobe at the Curtin University of Technology, using standard operating conditions (2 nA primary  $\text{O}^{2-}$  beam,  $20\text{ }\mu\text{m}$  analytical spot size, mass resolution ca. 5000). For magmatic zircons a 7-scan duty cycle was used and for detrital grains a 5-scan duty cycle was used. The common Pb component was estimated from  $^{204}\text{Pb}$  counts, assuming a typical terrestrial common Pb composition for the indicated age (Stacey and Kramers, 1975). Accumulated data for the CZ3 standard were used to correct for Pb/U elemental fractionation. Data reduction was carried out using SQUID v 1.02 and ISOPLOT v 2.49 by Ludwig (2001a,b). Measured isotopic ratios and calculated ages for individual spot analyses are given in Table 1. Concor-

dia plots of results are shown in Fig. 7. Ages are quoted in the text with  $1\sigma$  errors (Table 2).

#### 3.2. Laser Ablation Microprobe ICP-MS U–Pb analysis

Laser Ablation Microprobe ICP-MS (LAM ICP-MS) method has been used to rapidly determine the age of a larger number of zircons grains that are larger than  $80\text{ }\mu\text{m}$ . LAM ICP-MS U–Pb analyses were performed in the GEMOC Key Centre at Macquarie University, Sydney, using a HP 4500 inductively coupled plasma quadrupole mass spectrometer (ICP-MS) attached to a custom-built laser ablation micro sampling system (Norman et al., 1996). The analytical procedures for the U–Pb dating are described in detail by Belousova et al. (2001). A fast scanning data acquisition protocol for each analysis of 3 min (1 min on background, 2 min on signal) is used to minimize noise. Ablation was carried out in He to improve sample transport efficiency, to provide more stable signals, and to give more reproducible U/Pb fractionation. Samples were analysed in “runs” of ca. 18 analyses which included 10 unknowns, bracketed beginning and end, by four analyses including the GEMOC standards GJ, Mudtank and 02123 zircon standards. The ablation pit was approximately  $50\text{ }\mu\text{m}$  in diameter.

#### 3.3. Geochemical techniques

Samples were dried in a hot oven overnight and fused into lithium borate glass disks for major oxides. The major oxides were analysed using a Philips PW1400 automatic X-ray fluorescence (XRF) spectrometer at The University of Western Australia. X-rays were generated from a rhodium X-ray tube operated at 50 kV and 50 mA.

Trace elements were determined using a Perkin-Elmer Sciex ELAN 6000 ICP-MS at the Guangzhou Institute of Geochemistry, Chinese Academy of Sciences. About 50 mg sample powders were dissolved in Teflon beakers using a  $\text{HF} + \text{HNO}_3$  mixture. An internal standard solution containing the single element Rh was used to monitor signal drift during counting. The USGS standards BCR-1 and G-2 were chosen for calibrating element concentrations of measured samples. Analytical precision for most elements was better than 2%. The detailed procedures for trace element analysis by ICP-MS were described by Li (1997). Major and trace element data are presented in Table 3. Nd isotopic compositions were determined using a Micro mass Isoprene MC-ICPMS at the Guangzhou Institute of Geochemistry. The analytical procedures are similar to those

Table 1

SHRIMP analysis of magmatic zircons obtained from samples 03KD524 (Laowushan Formation) and 03KD531 (Heishantou Formation)

	U (ppm)	Th (ppm)	Th/U	f206 (%)	$^{207}\text{Pb}/^{206}\text{Pb} \pm \% \text{error} (1\sigma)$	$^{206}\text{Pb}/^{238}\text{U} \pm \% \text{error} (1\sigma)$	Apparent age Ma $^{207}\text{Pb}/^{206}\text{Pb} \pm 1\sigma$
Session 1032KD524							
524-1	64	27	0.43	0.12	$0.0774 \pm 2.1341$	$0.2223 \pm 2.4406$	$1350 \pm 74$
524-2	453	267	0.61	0.00	$0.0775 \pm 0.5959$	$0.2001 \pm 2.1095$	$1176 \pm 27$
524-3	295	178	0.62	0.06	$0.0891 \pm 1.0755$	$0.2347 \pm 2.0380$	$1381 \pm 48$
524-4	193	73	0.39	0.00	$0.1420 \pm 1.1211$	$0.4590 \pm 2.0532$	$2520 \pm 75$
524-5	1009	19	0.02	0.01	$0.0870 \pm 2.3257$	$0.1240 \pm 2.5741$	$1292 \pm 196$
524-6	537	426	0.82	0.04	$0.0769 \pm 0.7073$	$0.1957 \pm 2.0975$	$1139 \pm 25$
524-7	249	59	0.24	0.00	$0.0772 \pm 0.7056$	$0.1832 \pm 2.0592$	$1194 \pm 43$
524-8	453	479	1.09	0.14	$0.0762 \pm 0.7434$	$0.1911 \pm 2.0328$	$1114 \pm 25$
524-9	264	252	0.99	0.07	$0.0789 \pm 0.8843$	$0.1885 \pm 0.9747$	$1170 \pm 18$
Session 2							
524-10	281	160	0.59	0.00	$0.0801 \pm 0.6384$	$0.1904 \pm 0.8889$	$1200 \pm 13$
524-11	96	48	0.52	0.00	$0.0794 \pm 0.9173$	$0.2055 \pm 1.0482$	$1182 \pm 18$
524-12	229	276	1.24	0.13	$0.0784 \pm 0.6955$	$0.1965 \pm 0.9267$	$1157 \pm 14$
524-13	278	222	0.83	0.01	$0.0800 \pm 0.7039$	$0.1866 \pm 0.8837$	$1197 \pm 14$
524-14	185	92	0.52	0.19	$0.0766 \pm 0.9711$	$0.1840 \pm 1.5309$	$1112 \pm 19$
524-15	502	363	0.75	0.06	$0.0791 \pm 0.4802$	$0.1909 \pm 0.8229$	$1174 \pm 10$
524-16	863	549	0.66	0.05	$0.0794 \pm 0.3925$	$0.1961 \pm 0.8033$	$1182 \pm 8$
524-17	119	156	1.35	0.24	$0.0774 \pm 1.0615$	$0.1947 \pm 1.0073$	$1131 \pm 21$
524-18	110	28	0.26	0.00	$0.0885 \pm 0.7558$	$0.2326 \pm 0.9961$	$1392 \pm 15$
03KD531							
531-1	808	543	1.54	0.91	$0.1628 \pm 2.5544$	$0.0716 \pm 1.6655$	$976 \pm 34$
531-3	43	65	0.69	0.52	$0.1772 \pm 2.6444$	$0.0684 \pm 1.8965$	$881 \pm 39$
531-4	224	346	0.67	0.03	$0.3329 \pm 2.4932$	$0.1162 \pm 0.4121$	$1899 \pm 7$
531-5	42	59	0.74	0.63	$0.1778 \pm 2.6556$	$0.0682 \pm 3.9276$	$874 \pm 81$
531-6	228	270	0.87	0.03	$0.1678 \pm 2.5193$	$0.0729 \pm 0.8400$	$1013 \pm 17$
531-7	294	307	0.99	0.15	$0.1657 \pm 2.5149$	$0.0720 \pm 1.1942$	$985 \pm 24$
531-8	1014	694	1.51	0.20	$0.1509 \pm 2.4905$	$0.0725 \pm 1.0436$	$1001 \pm 21$
531-9	147	212	0.72	0.00	$0.1698 \pm 2.5218$	$0.0743 \pm 1.0656$	$1050 \pm 21$
531-10	103	124	0.86	0.23	$0.1715 \pm 2.5726$	$0.0699 \pm 2.1108$	$926 \pm 43$
531-11	114	141	0.84	0.11	$0.4357 \pm 4.0702$	$0.1465 \pm 2.3114$	$2306 \pm 40$
531-12	177	149	1.23	0.15	$0.1740 \pm 2.5438$	$0.0708 \pm 1.4452$	$952 \pm 30$
531-13	200	192	1.07	0.07	$0.1681 \pm 2.5259$	$0.0721 \pm 1.4267$	$988 \pm 29$
531-14	122	109	1.16	0.00	$0.1747 \pm 2.5671$	$0.0722 \pm 1.1222$	$991 \pm 23$
531-15	63	81	0.81	0.36	$0.2429 \pm 2.6210$	$0.0845 \pm 2.7981$	$1305 \pm 54$
531-16	105	141	0.77	0.37	$0.1683 \pm 2.5577$	$0.0694 \pm 2.2540$	$911 \pm 46$
531-17	49	61	0.83	0.13	$0.1774 \pm 2.6699$	$0.0712 \pm 2.2898$	$963 \pm 47$

described by Li et al. (2004). Nd fraction was separated by HDEHP-coated Kef columns. The aqueous Nd solution was taken up in 2%  $\text{HNO}_3$  and introduced into the MC-ICPMS using a Meinhard glass nebulae with an uptake rate of 0.1 ml/min. Measured  $^{143}\text{Nd}/^{144}\text{Nd}$  ratios were normalized to  $^{146}\text{Nd}/^{144}\text{Nd}=0.7219$ . The Isoprene MC-ICPMS was operated in static mode, and yielded  $^{143}\text{Nd}/^{144}\text{Nd}=0.512125 \pm 11$  ( $2\sigma$ ) on 14 runs for the Shin Eton JNdi-1 standard during the courses of this study. The reported  $^{143}\text{Nd}/^{144}\text{Nd}$  ratios were further adjusted to the Shin Eats JNdi-1 standard of  $0.512115 \pm 7$  ( $2\sigma_m$ ). Sm–Nd isotopic data are listed in Table 4.

## 4. Geochronological results

### 4.1. Zircon U–Pb data from tuff units

Zircon separates from two tuffaceous samples were analysed in order to constrain the depositional age of the successions. Sample 03KD531 was collected from the Heishantou Formation near the town of Ershan ( $102.172^\circ\text{E}$ ,  $24.248^\circ\text{N}$ ). Sample 03KD524 was from a tuffaceous unit within the rocks that we termed the Laowushan Formation ( $102.076^\circ\text{E}$ ,  $24.595^\circ\text{N}$ ). Zircons from these rocks are slightly pink in colour and their CL images show regular oscillatory growth zoning. The



Table 2  
Summary of apparent  $^{207}\text{Pb}/^{206}\text{Pb}$  ages of concordant (95–105%) detrital zircon data

Age (Ma)	Laowushan Formation (24°35.545'N, 102°04.184'E) <sup>a</sup> SHRIMP <sup>b</sup>	Kunyang Group			Huili Group	
		Liubatang Formation (24°41.072'N, 102°18.301'E) <sup>a</sup> LAM-ICPMS <sup>b</sup>	Yinmin Formation (26°15.623'N, 102°57.260'E) <sup>a</sup> SHRIMP <sup>b</sup>	Meidang Formation (26°15.626'N, 102°57.260'E) <sup>a</sup> SHRIMP <sup>b</sup>	Hekou Formation (26°15.623'N, 102°57.260'E) <sup>a</sup> LAM-ICPMS <sup>b</sup>	SHRIMP <sup>b</sup>
1000		968 ± 15 (2, 0.15) 1009 ± 8 (6, 1.01) 1251 ± 10				
1300	1193 ± 15 1354 ± 25 (2, 1.3)	1602 ± 18 (5, 1.2) 1732 ± 11 (2, 0.04) 1800 ± 23 (4, 2.3) 1864 ± 7 (7, 0.54) 1895 ± 7 (9, 1.07) 2008 ± 8	1625 ± 36 1885 ± 9		1400 ± 13 1825 ± 13 (2, 1.8)	1800 ± 5 1846 ± 9 (2, 0.71) 1917 ± 6 1943 ± 6
2200	2233 ± 9 (2, 0.91) 2284 ± 13 (7, 0.074) 2346 ± 8 (5, 0.81) 2398 ± 13 (4, 0.54) 2707 ± 4 (2, 0.31)		2736 ± 5 (12, 0.45)		2385 ± 13 (2, 0.14)	2239 ± 9 (2, 0.71) 2328 ± 7 2380 ± 16
3000				3034 ± 8 3364 ± 8 3575 ± 9 (2, 0.27)	2668 ± 8	2798 ± 5 3051 ± 9

Apparent ages of single concordant analyses with  $1\sigma$  error, weighted mean ages of two or more analyses are followed by (in parentheses) the number of analyses and MSWD of calculated mean.

<sup>a</sup> Location.

<sup>b</sup> Method.

Table 3

Major and trace element analyses of volcanic rocks sampled from the Kunyang Group and the Laowushan Formation

	Alkali basalt							Tuff	Basalt, (Louxue Mine)
	03KD516 (24°35.939', 102°04.815') <sup>a</sup>	03KD518 (24°35.685', 102°04.814') <sup>a</sup>	03KD520 (24°35.399', 102°03.957') <sup>a</sup>	03KD521 (24°35.472', 102°04.026') <sup>a</sup>	03KD523 (24°35.545', 102°04.184') <sup>a</sup>	03KD527 (24°35.009', 102°04.783') <sup>a</sup>	03KD528 (24°35.062', 102°04.792') <sup>a</sup>	03KD531 (24°35.939', 102°04.815') <sup>a</sup>	33KD476
SiO <sub>2</sub>	58.22	54.83	48.08	54.40	56.22	55.70	51.40	47.51	44.55
TiO <sub>2</sub>	2.15	2.06	2.78	2.78	1.97	2.23	2.89	2.22	1.98
Al <sub>2</sub> O <sub>3</sub>	20.12	14.24	15.70	15.91	11.03	14.26	18.61	16.42	11.87
FeO <sup>t</sup>	9.65	9.85	9.16	12.40	12.18	14.63	16.76	14.10	24.95
MnO	0.02	0.06	0.18	0.06	0.09	0.07	0.03	0.14	0.10
MgO	3.47	4.42	3.53	4.42	3.32	7.00	4.09	2.42	4.39
CaO	0.48	9.38	14.58	5.10	10.55	2.33	0.15	9.23	5.85
Na <sub>2</sub> O	1.52	2.30	0.64	0.45	0.87	0.03	0.04	4.12	5.37
K <sub>2</sub> O	4.01	2.36	4.85	4.28	3.14	3.62	5.88	3.36	0.72
P <sub>2</sub> O <sub>5</sub>	0.35	0.50	0.50	0.18	0.62	0.13	0.13	0.48	0.22
Mg#	26.46	30.95	27.84	26.29	21.43	32.37	19.63	14.63	14.98
LOI	6.16	9.10	12.62	7.37	9.32	5.50	8.41	8.29	4.66
Sc	15.09	14.49	20.28	18.77	11.55	14.67	13.80	14.77	25.41
V	247.60	148.80	210.60	84.67	125.50	104.20	99.90	104.80	339.20
Cr	105.80	111.80	104.90	90.59	44.47	85.59	60.82	179.40	56.21
Co	30.99	27.96	20.54	26.49	21.39	40.78	38.57	25.69	55.84
Ni	75.50	67.90	67.89	65.06	50.27	86.16	94.08	91.84	57.10
Rb	77.69	45.28	113.10	83.87	54.99	91.38	105.00	66.53	18.43
Ba	199.10	380.00	316.40	199.50	591.10	421.90	344.80	767.50	24.27
Th	3.92	3.53	2.02	1.88	1.56	2.07	3.82	3.20	2.55
U	2.19	0.61	0.87	0.15	0.29	0.58	0.46	0.51	0.56
Nb	46.27	36.61	31.12	28.03	19.75	24.74	51.08	39.84	14.99
Ta	3.29	2.60	2.27	2.10	1.31	1.86	3.18	2.59	0.90
La	50.60	38.07	17.92	26.77	20.19	31.30	34.11	40.97	8.65
Ce	107.20	77.13	45.33	57.01	44.60	65.27	68.47	78.56	21.34
Pr	14.01	9.73	5.67	7.36	6.10	8.47	8.60	10.27	3.10
Sr	36.58	23.10	4.20	3.64	69.68	49.62	4.53	354.20	26.58
Nd	57.69	37.19	22.69	29.49	27.96	34.97	32.86	40.03	14.34
Zr	311.00	288.10	238.80	213.90	122.80	211.00	298.60	213.20	123.40
Hf	7.83	6.57	6.00	4.45	3.01	5.14	6.75	4.96	2.95
Sm	9.59	5.54	3.40	4.83	5.16	6.53	5.14	6.69	3.21
Eu	2.95	1.26	0.92	1.53	1.73	2.11	1.38	2.12	0.88
Gd	6.96	3.60	1.88	3.20	4.57	5.72	3.26	5.28	3.65
Tb	1.07	0.55	0.32	0.51	0.67	0.85	0.50	0.84	0.70
Dy	5.14	3.03	1.96	2.73	3.41	4.35	2.79	4.19	4.61
Y	19.38	14.74	9.42	10.86	14.50	20.59	12.87	18.19	27.25
Ho	0.85	0.58	0.41	0.50	0.62	0.74	0.55	0.73	1.00
Er	2.00	1.58	1.19	1.28	1.63	1.83	1.48	1.85	2.76
Tm	0.24	0.20	0.17	0.17	0.23	0.22	0.20	0.25	0.42
Yb	1.36	1.23	1.01	1.03	1.44	1.37	1.19	1.49	2.56
Lu	0.19	0.18	0.15	0.15	0.22	0.20	0.18	0.23	0.31

All analyses are recalculated to 100% on volatile free basis.

<sup>a</sup> (Latitude, Longitude).

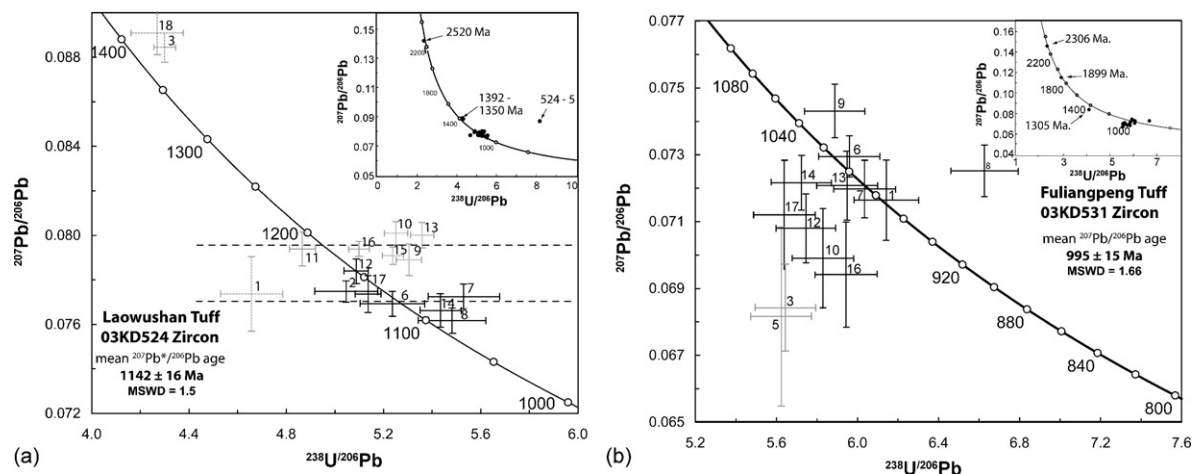


Fig. 7. Terra–Wasserburg diagrams for (a) sample 03KD524 and (b) sample 03KD531. Error crosses indicate  $1\sigma$  errors.

grains have low to moderate concentrations of U (mostly 140–500 ppm) and Th (mostly 49–292 ppm). All analyses were plotted using Terra–Wasserburg plots to better represent the measured, rather than the calculated values (Fig. 7).

Analyses of sample 03KD524 were carried out in two sessions (session 1, spots 1–9 and session 2, spots 10–18) on a single mount. Four analyses (spots 3, 4, 5 and 18) were excluded from age calculations as they were determined to be xenocrystic on the basis of morphology and significantly older apparent ages. These grains include one of Archean ( $^{207}\text{Pb}/^{206}\text{Pb}$  age; 2520 Ma) and two of mid Mesoproterozoic ages ( $^{207}\text{Pb}/^{206}\text{Pb}$  ages; 1392–1350 Ma). Two discrete age populations are shown in Fig. 7a. The eldest one, shown in light grey is represented by six analyses (spots 9, 10, 11, 13, 15 and 16), giving a weighted average  $^{207}\text{Pb}/^{206}\text{Pb}$  age of  $1180 \pm 9$  Ma (MSWD = 0.62). The youngest population consists of seven analyses (spots 2, 6, 7, 8, 12, 14 and 17) with a weighted mean  $^{206}\text{Pb}/^{207}\text{Pb}$  age of  $1142 \pm 16$  Ma (MSWD = 1.5 Ma), which we interpret as the depositional age of the tuff unit.

All data for sample 03KD531 was collected in a single session and is listed in Table 1 and plotted on Fig. 7b. Three grains (spots 4, 11 and 15) were excluded as their morphology and ages indicate they are xenocrystic grains with 2306, 1899 and 1305 Ma concordant ages. Two grains differ from the main population (spots 3 and 5) with apparent  $^{207}\text{Pb}/^{206}\text{Pb}$  ages of  $881 \pm 81$  and  $874 \pm 39$  Ma, very low uranium (65 and 59 ppm) and inversely discordant. Including these two grains in an age calculation, gives a weighted mean  $^{207}\text{Pb}/^{206}\text{Pb}$  age of  $990 \pm 25$  Ma ( $n = 13$ , MSWD = 2.2). The corresponding  $^{206}\text{Pb}/^{238}\text{U}$  apparent ages are dispersed beyond analytical precision of this weighted mean, yielding an age range of  $\sim 1052$ –906 Ma.

On a Terra–Wasserburg diagram (Fig. 7b), it is evident that five of the analyses with the oldest apparent ages are also inversely discordant. All analyses show a negative correlation between apparent  $^{206}\text{Pb}^*/^{238}\text{U}$  and U concentration, with the youngest apparent  $^{206}\text{Pb}^*/^{238}\text{U}$  ages being in good agreement with the mean  $^{207}\text{Pb}/^{206}\text{Pb}$  age. This may suggest either the presence of unsupported radiogenic Pb (Mattinson et al., 1996), labile

Table 4

Sm–Nd isotopic data for the volcanic rocks sampled from the Kunyang Group and the Laowushan Formation

Sample	Sm	Nd	$^{147}\text{Sm}/^{144}\text{Nd}$	$^{143}\text{Nd}/^{144}\text{Nd}$	$\pm 2\sigma$ m	CHUR	$T_{\text{DM}}$	$\varepsilon\text{Nd}(0)$	$\varepsilon\text{Nd}(0.9)$	$\varepsilon\text{Nd}(1.1)$
03KD516	9.59	57.69	0.1005	0.511873	0.000008	1.21	1.55	−14.92	−2.75	−0.89
03KD518	5.54	37.19	0.1490	0.511766	0.000006	1.25	1.55	−17.00	−4.75	−1.44
03KD520	3.40	22.69	0.0906	0.511872	0.000012	1.10	1.44	−14.95	−1.50	0.55
03KD521	4.83	29.49	0.0990	0.511946	0.000010	1.08	1.45	−13.50	−1.12	0.77
03KD523	5.16	27.96	0.1115	0.512019	0.000009	1.11	1.51	−12.07	−1.28	0.36
03KD527	6.53	34.97	0.1130	0.512013	0.000009	1.14	1.54	−12.20	−1.59	0.02
03KD528	5.14	32.86	0.0946	0.511917	0.000010	1.08	1.43	−14.06	−1.13	0.84
03KD531	6.69	40.03	0.1011	0.511972	0.000009	1.06	1.44	−12.99	−0.87	0.61
03KD476	3.21	14.34	0.1355	0.512261	0.000011	0.94	1.50	−7.36	0.40	1.27

radiogenic lead within the amorphous zones of zircon grains (Wiedenbeck, 1995) or the enhanced sputtering of Pb relative to U as a result of radiation-induced damage to the grains microstructure (McLaren et al., 1994). The inversely discordant grains have the lowest U contents (64–149 ppm) and low birefringence; these features may suggest presence of an unsupported or labile radiogenic Pb component rather than radiation damage. A weighted average (MSWD = 0.4)  $^{207}\text{Pb}/^{206}\text{Pb}$  age of  $1001 \pm 22$  Ma is calculated from the four most concordant grains (1, 6, 7 and 13). This age varies only slightly to the weighted average ( $n = 11$ , MSWD = 1.66)  $^{207}\text{Pb}/^{206}\text{Pb}$  age of  $996 \pm 15$  Ma calculated from all, but the two most discordant analyses (i.e. spots 3 and 5) and is taken as the best age estimation of the tuff unit.

Our new isotopic ages indicate that the volcanic rocks of the Laowushan Formation (sample 03KD524) are about 140 Ma older than the Heishantou Formation (sample 03KD531 from the Fuliangpeng Member of this formation). They therefore could not be the lateral equivalents of the Fuliangpeng Member in the Heishantou Formation. We thus suggest that this volcanic unit near the Laowushan village represents an older tectonostratigraphic unit separate to the rocks of the Kunyang Group, here termed the Laowushan Formation.

#### 4.2. Detrital zircon analyses

U–Pb ages were determined for 190 detrital zircon grains from five samples collected from the late Mesoproterozoic–earliest Neoproterozoic successions outcropping along the western South China Block. Samples include one from the newly defined Laowushan Formation, three from the previously defined Kunyang Group and two from the equivalent rock units in the Huili Group (Fig. 4). These data have been used to determine the detrital provenance and maximum ages of sedimentation. All data are presented on a Terra–Wasserburg diagram (Fig. 8) and the concordant analyses are plotted as cumulative probability curves (Fig. 9). The ages of subpopulations identified from plots are quoted as age ranges and ages from individual analyses are quoted with  $1\sigma$  errors.

As only a relatively small number of zircons were analysed from the samples of the Yinmin shale (02KD008) and Tongan shale (03KD535), a less precise determination of the age populations can be made. Zircons from two quartzite samples (the Liubatang Formation: 02KD178; the Hekou Formation: 03KD458) were analysed using LAM-ICPMS at the GEMOC Laboratory at Macquarie University. The small ( $<60\ \mu\text{m}$ )

zircon grains from samples 02KD008, 03KD458 and 03KD527 were analysed using the SHRIMP II at Curtin University. An apparent  $^{206}\text{Pb}/^{207}\text{Pb}$  age is presented for each analysis with  $1\sigma$  error (see supplementary data).

##### 4.2.1. Laowushan Formation

Fifty-three detrital zircons separated from a fine-grained sandstone unit in the Laowushan Formation were analysed (Figs. 8a and 9a). The zircons show only a small Archean population including a single 2861 Ma grain, two 2707 Ma and a single 2607 Ma grains. The ages of these grains are similar to those of granites found in the Archean basement rocks of the Yangtze Block (e.g. the Kongling Complex; Qiu et al., 2000). Two separate populations of early Paleoproterozoic zircons are present: a small ca. 2398–2321 Ma population and a larger ca. 2291–2216 Ma population. Most early Paleoproterozoic grains are magmatic in origin, but two grains have low Th/U ratios suggesting a metamorphic origin (e.g. Rubatto and Gebauer, 2000) at 2229 Ma (Th/U = 0.10) and 2002 Ma (Th/U = 0.06). No 2400–2200 Ma source rocks have yet been identified in the Yangtze region. The absence of 1700–1600 Ma grains suggest little input was derived from local Paleoproterozoic basement rocks like the Dahongshan Group.

A small population of Mesoproterozoic zircons including two grains with 1394 and 1434 Ma ages are similar in age to granites found on Hainan Island and detrital grains found in Kunyang Group equivalent quartzites analysed by Li et al. (2002b). As there is no known source region on the Yangtze Block for such grains, their presence is consistent with a possible Cathaysian source at this time (Li et al., 2002b). The youngest single zircon has an apparent age of  $1193 \pm 15$  Ma, which is within error of the xenocrystic grains identified in the tuff sample (03KD524) from the same formation.

##### 4.2.2. Meidang Formation

Sample 03KD535 was collected from rocks mapped as the Tongan Formation (1:200,000 map sheet; Huili, 1967), which have been correlated with fine-grained shale unit found in the Meidang Formation of the Kunyang Group. Ten small ( $\sim 50\ \mu\text{m}$ ) well-rounded zircons were separated from this rock of which only five gave concordant ages (Figs. 8b and 9b). The age distribution of these zircons is Archean to early Paleoproterozoic. Three magmatic zircons with ages of 3576–3364 Ma are the oldest crustal material yet found in South China. Two slightly younger zircons gave late Archean ages: one being a 2961 Ma metamorphic grain

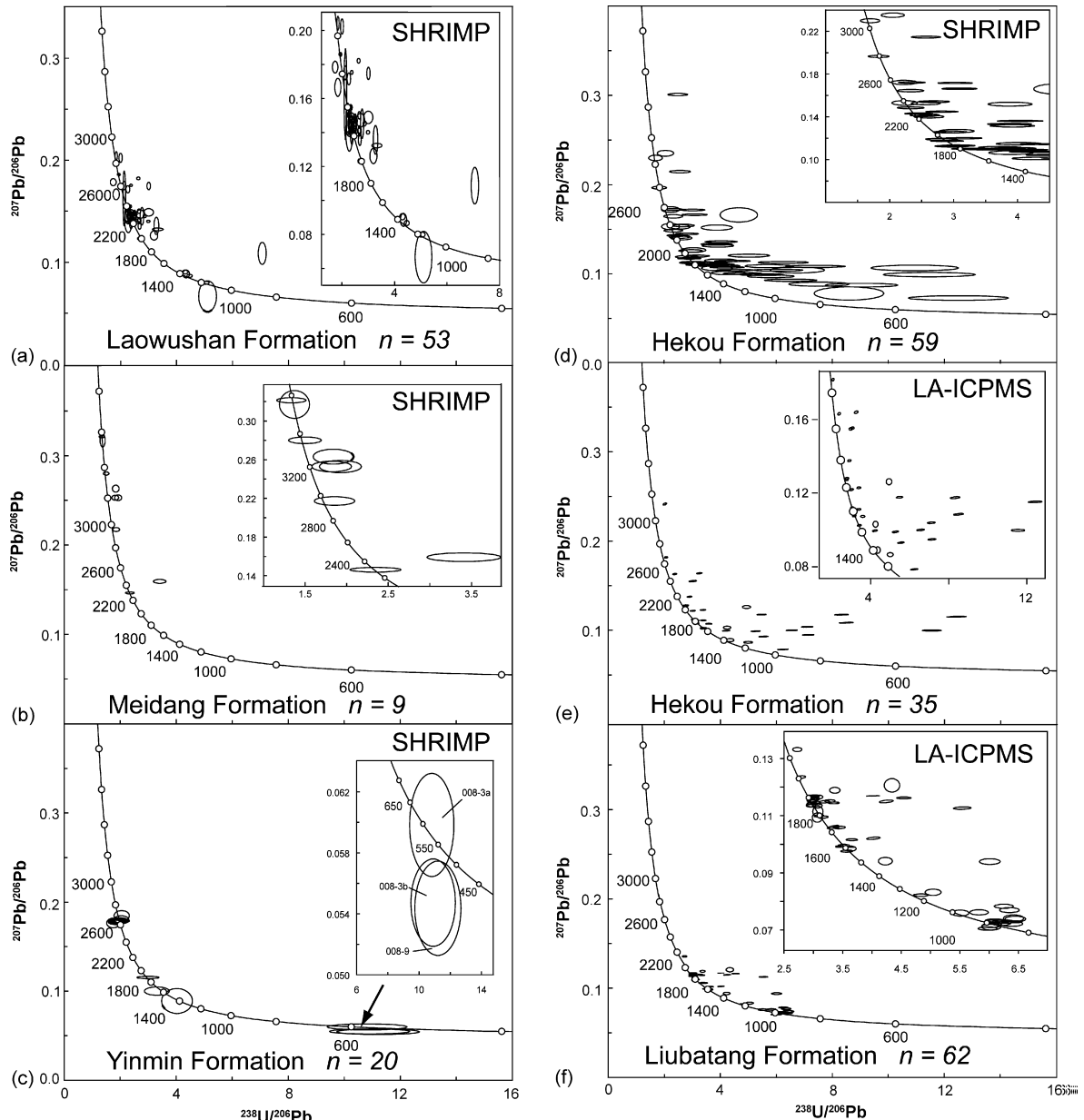


Fig. 8. (a–f) Terra–Wasserburg diagrams of all detrital zircon U–Pb analyses for the late Mesoproterozoic and earliest Neoproterozoic sedimentary rocks.

(U/Th=0.03) and the other being a 2303 Ma magmatic grain.

#### 4.2.3. Yinmin (Limahe) Formation

Sample 02KD008 was from a fine-grained shale member of the Yinmin Formation (or as the Limahe Formation, 1:200,000 Huili geological map sheet, 1967). This sample contained only 19 small (<50  $\mu\text{m}$ ) zircons and three larger grains (~80  $\mu\text{m}$ ): 13 gave concordant ages, including a late Archean (2657–2627 Ma) pop-

ulation, two Paleoproterozoic (1885–1625 Ma) grains and an early Mesoproterozoic (ca. 1402 Ma) grain (Figs. 8c and 9c). These data suggest a dominantly Archean provenance, and the presence of single ca. 1400 Ma grain suggests a possible Cathaysian input. Two of the larger grains (Fig. 8c, grains 3 and 9) gave discordant apparent ages younger than the age of this formation. This may suggest isotopic disturbance as indicated by the inversed discordance of the grains, or the presence of excess Pb.



#### 4.2.4. Hekou Formation

The meta-sedimentary rocks of the Hekou Formation are exposed in southern Sichuan Province. The rocks are variably metamorphosed to upper greenschist facies and have previously been correlated to the Paleoproterozoic rocks of the Dahongshan Group (e.g. Chen and Ran, 1992).

The analyses of 59 (SHRIMP; Figs. 8d and 9d) and 35 (LAM-ICMS; Figs. 8e and 9e) zircons from the quartzite at the Lala Copper Mine (sample 03KD458) show a large discordant population with only 18 concordant grains, making detailed interpretation difficult. The two grains (ca. 3051–2797 Ma) are significantly older than the other grains present in this sample. Two Paleoproterozoic age populations are also present. The oldest population ( $n=4$ ) of ca. 2360–2070 Ma has a similar age range to the largest population found in the Laowushan Formation. The presence of a larger Paleoproterozoic population ( $n=8$ ) of ca. 1942–1800 Ma demonstrates a change in provenance from that of the Laowushan Formation. Two younger grains of 1759–1669 Ma are close in age to the Paleoproterozoic rocks found locally in the Dahongshan Group. A single 1400 Ma grain suggests these rocks are younger than the Dahongshan Group and may represent a metamorphosed equivalent of the Kunyang Group rather than the Paleoproterozoic Dahongshan Group as suggested previously.

#### 4.2.5. Liubatang Formation

The Liubatang Formation is found at the stratigraphic top of the Kunyang Group. The type section of this formation contains mature quartz-rich sediments with some carbonate and shale. The unimodal cross-bedded quartz sandstones, conglomerate and gravels suggest a fluvial environment (Fig. 6). Sample 02KD178 was taken from the quartz sandstone at the base of the formation.

The analysed grains show no Archean provenance, contrasting to the lower stratigraphic units of the Kunyang Group (Figs. 8f and 9f). The oldest grains in this sample are Paleoproterozoic in age and the largest ( $n=9$ ) single population has an age range of 1909–1880 Ma. Granites of this age range are found intruding the Kongling area of the Yangtze Block (Qiu et al., 2000). Three slightly younger Paleoproterozoic populations of 1874–1857 Ma ( $n=7$ ), 1843–1789 Ma ( $n=4$ ) and 1734–1730 Ma ( $n=3$ ) are also present. A late Paleoproterozoic–early Mesoproterozoic population (1663–1507 Ma,  $n=5$ ) is similar to the age of the Dahongshan Group metavolcanic rocks, suggesting possible erosion of these rocks at this time. A late Mesoproterozoic population ( $n=4$ , 1275–1251 Ma) is slightly older than the volcanic rocks found in the Laowushan

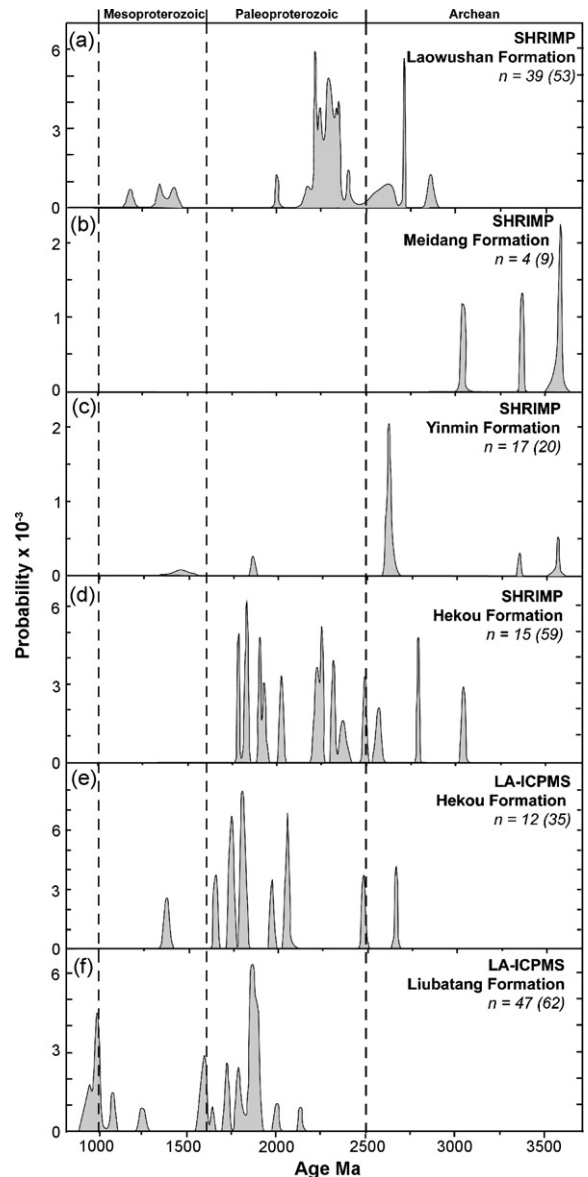


Fig. 9. (a–f) Histogram plots of the apparent  $^{206}\text{Pb}/^{207}\text{Pb}$  ages of concordant (90–110%) detrital zircon analyses from the late Mesoproterozoic–earliest Neoproterozoic sedimentary rocks (Plotted using AgeDisplay v.2; Sircombe, 2003).

Formation, suggesting reworking of this early basin fill at the time. A late Mesoproterozoic population ( $n=6$ , 1023–993 Ma) provides a weighted mean age of  $1009 \pm 8$  Ma (MSWD = 1.01) which is within error of the age obtained for the tuff sample of the Heishantou Formation (03KD531). The youngest population of early Neoproterozoic aged grains ( $n=2$ , 964–970 Ma) provides a weighted mean age of  $968 \pm 15$  Ma which may be interpreted as the maximum age of deposition for the Liubatang Formation.

## 5. Geochemistry

The results of chemical analyses of volcanic rocks are presented in Table 3. Eight basaltic samples were collected from the Laowushan Formation. A tuffaceous sample was collected from the upper Fuliangpeng Member of the Heishantou Formation, and another basaltic sample from the Yinmin Formation.

The Laowushan basalts are altered, with most ferromagnesian minerals being altered to chlorite or clay minerals although they still retain the grain boundaries. The feldspars are small (0.25–1 mm) lath-like grains, which are totally albitised. The basalts are vesicular (3–15 mm diameter) with the cavities being infilled with either carbonate or chlorite. The volcanoclastic rocks include tuffs and volcanic sandstones with fine lithic grains of volcanic rocks. The volcanic breccias contain fragments of basalt and volcanoclastic rocks (20–150 mm). The matrix of these rocks contains finer grained fragments (<10 mm) of these volcanic rocks and a carbonate cement.

The Yinmin Formation basalt is also altered, containing a fine-grained matrix of feldspar and biotite. The more ferromagnesian minerals are pseudomorphed by epidote and chlorite. The basalts have amygdalae that are infilled with biotite, chlorite and pyrite. The Fuliangpeng tuff is a fine-grained grey rock containing mineral grains of feldspar, mica and chloritised ferromagnesian minerals.

### 5.1. Major and trace element chemistry

All analyses have been recalculated to 100% on a volatile free basis due to the high volatile content of these rocks (LOI = 4.62–12.62) indicative pervasive alteration. Elements which are mobile during alteration include SiO<sub>2</sub>, Na, K and the low field strength elements (e.g. Humphris and Thompson, 1978), whereas the high field strength elements and the rare earth elements (REE) are relatively immobile in all but the most severe hydrothermal alteration (Pearce, 1975; Wood et al., 1979). For this reason only high field strength elements Ti, Zr, Y, Nb, Ta, Hf, Th and REE have been used in the discussion of the magmatic affinities and petrogenesis of these mafic volcanic rocks.

For the classification of these altered volcanic rocks, the Zr/TiO<sub>2</sub> versus Nb/Y plot of Winchester and Floyd (1977) has been used (Fig. 10). The Laowushan rocks plot on the alkali basalt–basanite fields of this diagram and the Fuliangpeng rocks plot in the alkali basalt field. Sample 03KD476 from the Yinmin Formation plots in the sub-alkaline basalt field.

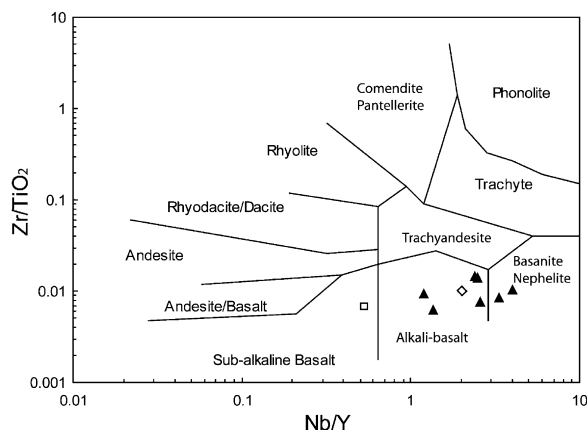


Fig. 10. Zr/TiO<sub>2</sub> vs. Nb/Y rock classification diagrams (Winchester and Floyd, 1977): (▲) Laowushan Formation; (□) Yinmin Formation; (◇) Fuliangpeng Member of Heishantou Formation.

The enrichment of high field strength elements (HFSE) in basaltic magmas can be a good indicator of tectonic environment (e.g. Pearce and Cann, 1971, 1973; Pearce, 1975). TiO<sub>2</sub> is generally >2 wt.% in the Laowushan rocks and sample 03KD531, typical of alkalic intraplate magmatism. Sample 03KD476 has slightly lower TiO<sub>2</sub> (1.87 wt.%). Most Laowushan basalts have high Zr values (211–442 ppm); one exception being 03KD522 which has slightly lower Zr (122 ppm). The Fuliangpeng tuff (03KD531) also has a high Zr value of 213 ppm, but the Yinmin Formation basalt (03KD476) has lower Zr (123 ppm).

The Ti/V ratios of all samples vary between 52 and 266, indicative of either continental alkaline basalt or ocean island basalt affinities (Shervias, 1982). When plotted on the tectonic discrimination diagrams defined by Wood (1980) and Pearce (1983), the volcanic rocks from the Laowushan and Fuliangpeng Formations plot in the within plate alkali basalt fields (Figs. 11 and 12). The Yinmin basalt sample plots outside these fields on both diagrams (Figs. 11 and 12) due to the lower Ta (0.9 ppm).

### 5.2. Rare earth elements

All samples from the Fuliangpeng basalts have uniform chondrite normalized REE patterns with slight LREE enrichment (La/Yb)<sub>N</sub> = 7.4–25.3 and La<sub>N</sub> = 75–213 (Fig. 13). Most samples show a very slight positive Eu anomaly (Eu/Eu\* = 0.95–1.18), however, samples 03KD530 (Eu/Eu\* = 0.63) and 03KD522 (Eu/Eu\* = 0.93) have very slight negative Eu anomalies. Sample 03KD476 has less LREE enrichment (La/Yb)<sub>N</sub> = 2.29 (La<sub>N</sub> = 36.5) and a larger negative Eu anomaly (Eu/Eu\* = 0.78). The depleted HREE rel-

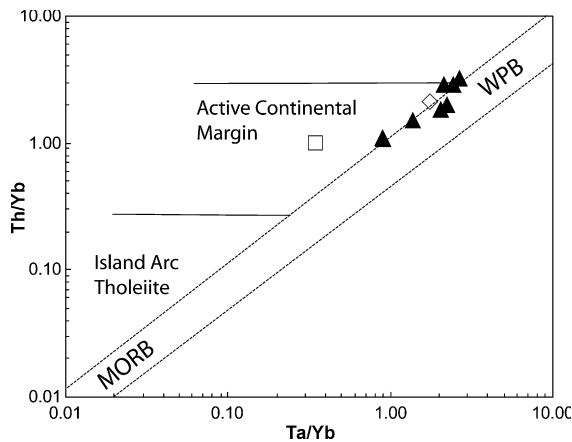


Fig. 11. Ta/Yb vs. Th/Yb tectonic discrimination diagram for basalts (Pearce, 1983): (▲) Laowushan Formation; (□) Yinmin Formation; (◇) Fuliangpeng Member of Heishantou Formation.

ative to LREE is apparent in the high ratios of  $(\text{Gd}/\text{Yb})_{\text{N}} = 1.17\text{--}4.24$ , which suggest a fractionated garnet-rich source (Frey et al., 1978).

When plotted on a primitive-mantle normalized trace element diagram (Fig. 14; Sun and McDonough, 1989) all samples have a fractionated pattern characterised by variable enrichment of the more incompatible trace elements with respect to primitive-mantle. Samples from the Laowushan Formation display mild to strong Nb–Ta enrichment (i.e. Nb/La varying between 0.79 and 3.46), similar to many alkali basalts from continental rifts or ocean islands without appreciable crustal contamination (e.g. Barrat et al., 1998; Rogers et al., 2000). Two samples (03KD521 and 03KD523) with the lowest Nb/La ratios are less enriched in Zr (122 and 213 ppm) and Th

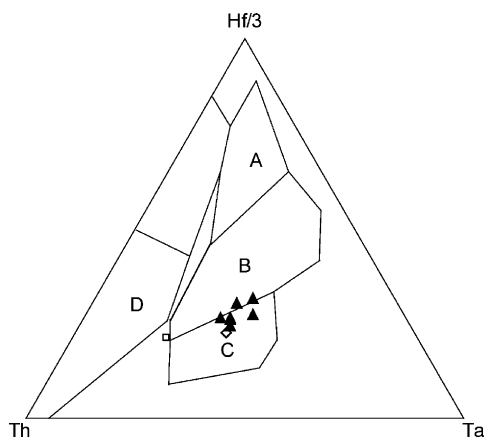


Fig. 12. Th–Hf/3–Ta tectonic discrimination plot for basalts (Wood, 1980). The fields are: (A) N-type MORB; (B) E-type MORB; (C) alkaline within plate basalts; (D) volcanic arc basalts and island arc tholeiites: (▲) Laowushan Formation; (□) Yinmin Formation; (◇) Fuliangpeng Member of Heishantou Formation.

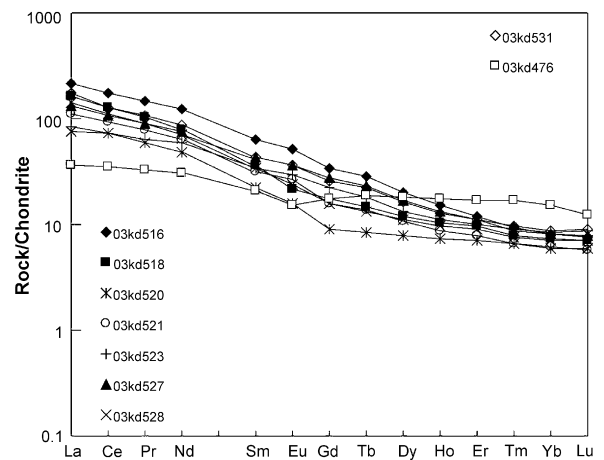


Fig. 13. Chondrite normalized REE diagram for basalts from the Laowushan Formation and Kunyang Group (Sun and McDonough, 1989).

(1.88 and 1.56 ppm) suggesting some contamination by a more sialic crust (e.g. Thompson et al., 1984; Li et al., 2002a; Moraes et al., 2003). Sample 03KD531 is depleted in Nb–Ta ( $\text{Nb}/\text{La} = 0.97$ ) and has a high Nb/Th ratio (12.45). Sample 03KD476 has significantly lower Nb/Th, suggesting more crustal contamination or different petrogenetic processes (e.g. Thompson et al., 1984). When plotted on a Th/Yb versus Ta/Yb diagram the Laowushan and Fuliangpeng samples plot in the within plate basalt field as defined by Pearce (1983). Sample 03KD476 plots away from the other samples with lower Ta/Yb ratio (0.35) and Th/Yb ratio (0.99), causing it to plot in the active continental margin field. The Yb/Ta versus Y/Nb ratios correlate positively, with samples

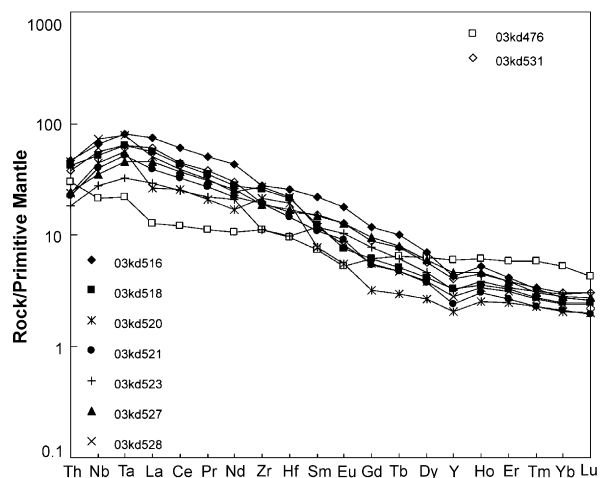


Fig. 14. Primitive-mantle normalized spider diagram for basalts from the Laowushan Formation and Kunyang Group (Sun and McDonough, 1989).

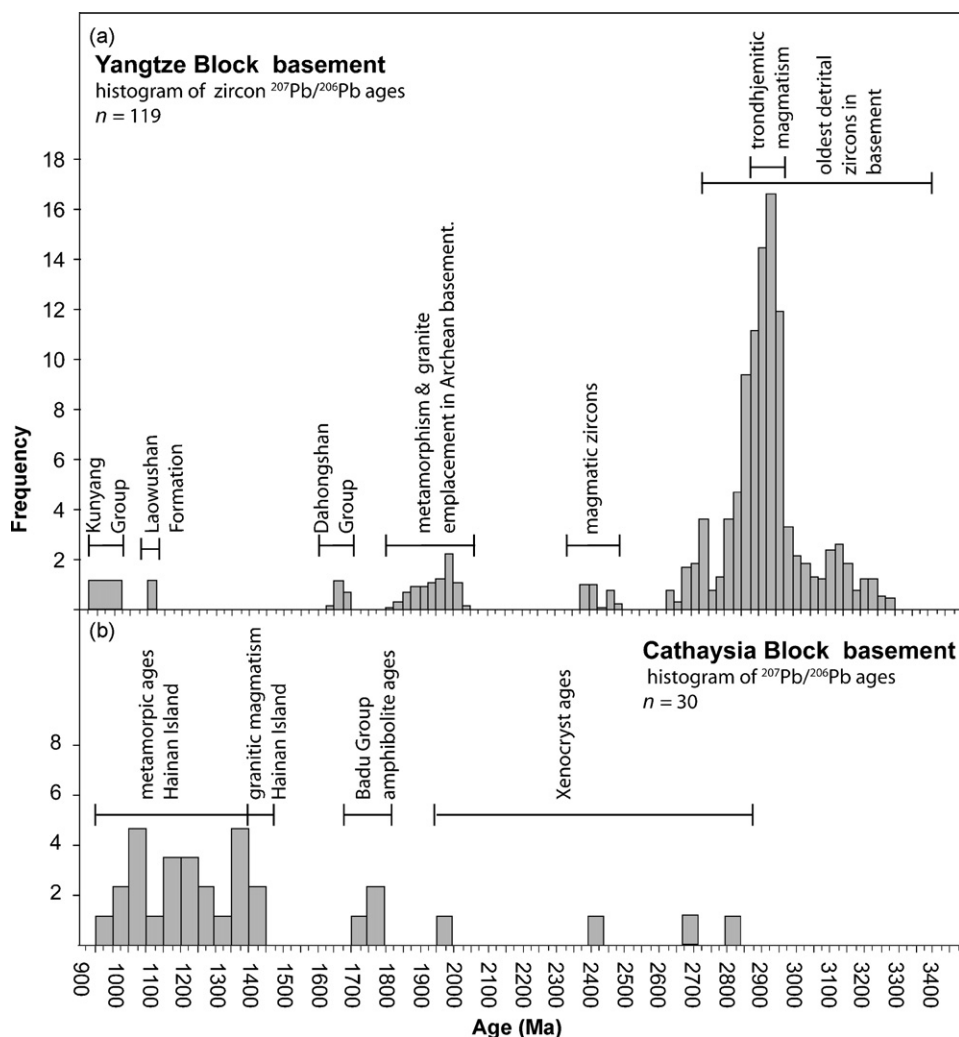


Fig. 15. Histogram distribution of concordant (90–110%)  $^{207}\text{Pb}/^{206}\text{Pb}$  (SHRIMP and LAM-ICPMS) for zircon analyses from the Pre-900 Ma basement rocks of (a) Yangtze Block (Qiu et al., 2000; Hu et al., 1991; Zhang et al., 2006) and (b) Cathaysia Block (Li, 1997; Li et al., 2002a,b). Histograms plotted using AgeDisplay v.2 (Sircombe, 2003).

03KD523, 03KD527 and 03KD476 having the highest ratios.

### 5.3. Nd isotopes

Nine selected samples were analysed for Nd isotopes, including seven from the Laowushan Formation, a tuff sample from the Fuliangpeng Member of the Heishantou Formation and a basalt sample from the Yinmin Formation (Table 4). The initial isotopic composition of samples for the Laowushan, Heishantou and Yinmin Formations are listed in the form of  $\epsilon\text{Nd}(T)$  for the ages of 1.1 and 0.9 Ga for comparison.

All samples have uniformly chondritic  $\epsilon\text{Nd}(T)$  values varying between  $-0.87$  and  $+0.84$ . The  $T_{\text{DM}}$  model

ages suggest a slightly older magmatic source than determined from the SHRIMP zircon geochronology. The CHUR model ages support the SHRIMP ages, and indicate that the Laowushan rocks are slightly older than the Kunyang Group rocks.

## 6. Discussion

Previous work in the region has largely favoured a long-lived rift model for explaining the alkaline volcanism, shallow marine sediments and stratiform copper mineral deposits (Yunnan, 1987; Wu et al., 1990; Zhang et al., 2003). New analytical data, including geochronology, detrital provenance, geochemistry and stratigraphy as presented in this paper, suggest that the traditionally

defined Kunyang Group consists of at least two tectonostratigraphic packages. Our new interpretation of tectonic significance of these rocks is presented below.

### 6.1. Petrogenesis of the Laowushan and Yinmin basalts

The geochemical characteristics of the Laowushan basalts are similar to modern alkali basalts found in continental rifts (e.g. Sengor et al., 1978; Dewey and Windley, 1988; Barrat et al., 1993, 1998; Pik et al., 1999; Rogers et al., 2000; Ritter et al., 2001), including the enrichment of incompatible elements and high field strength elements such as  $\text{TiO}_2$  (mostly  $>2$  wt.%), Zr (122.80–442.10 ppm), Ta (1.31–3.29) and Th (1.56–3.92 ppm), the enrichment of LREE ( $(\text{La}_N = 75\text{--}213)$ ) and the HREE fractionation ( $(\text{Gd/Yb})_N > 1$ ). The fractionation of the HREE in these basalts suggests a magma generated from a garnet rich source. Crustal materials might have been involved in

the origin of the basaltic rocks in view of the variation in  $\epsilon\text{Nd}$  values from  $-0.89$  to  $0.84$ . These near zero, chondritic  $\epsilon\text{Nd}$  values can be interpreted as the result of mixing between mantle-derived magmas with variably positive  $\epsilon\text{Nd}$  values and continental crust components with variably negative  $\epsilon\text{Nd}$  values. Geochemical features, such as high Nb/La ( $>1$ ) and Nb/Th ( $>10$ ) ratios, preclude a significant involvement of crustal components in the basalts. Thus, the Laowushan basalts were likely derived from a relatively less depleted mantle reservoir (either subcontinental lithosphere or a plume source), and the basaltic magmas were assimilated with minor crustal components.

The Yinmin basalt (03KD476) is from a stratigraphically higher level than both the Heishantou Formation tuffs and the Laowushan basalts. It is chemically distinct from these rocks. The higher Zr/Ti ratio (52.96) suggests magma generated in an intraplate setting, but the lower Nb/Y ratio (0.55) indicates lower alkalinity than the Laowushan rocks. A flatter REE and less enriched

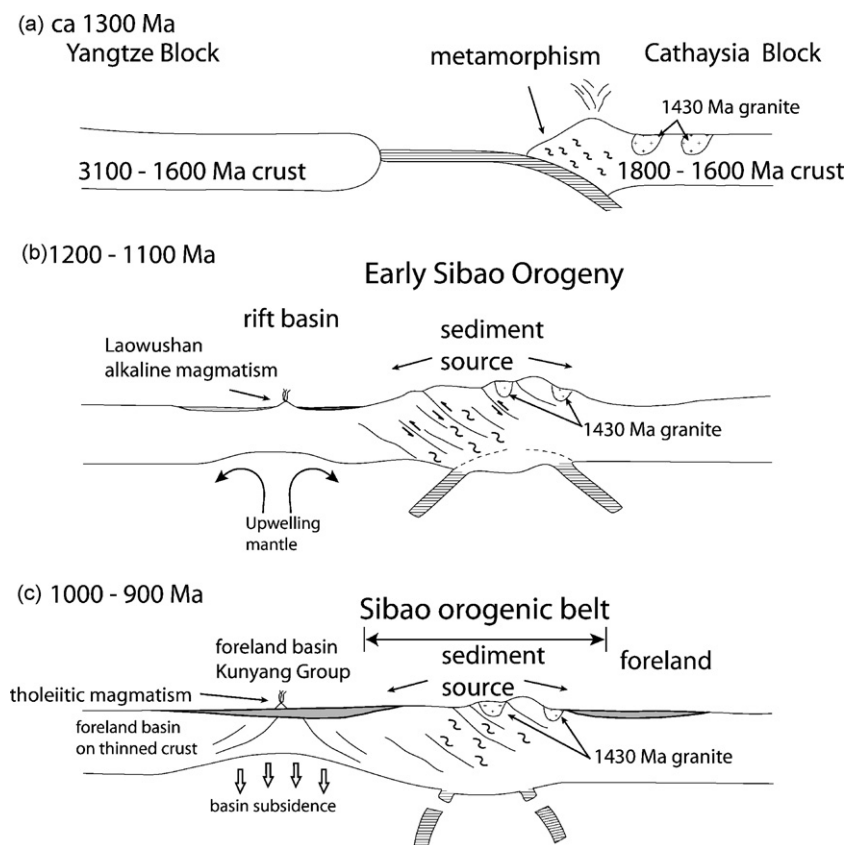


Fig. 16. A schematic cross-section showing the collision between the Yangtze and Cathaysia Blocks during the late Mesoproterozoic–earliest Neoproterozoic. (a) An ocean basin separates the Yangtze and Cathaysia Blocks. Metamorphism recorded on the Cathaysia Block suggests the presence of an active margin. (b) The initial collision occurring at the southern tip of the Yangtze Block. Intracontinental rifting occurs at a high angle to this collision. (c) The Yangtze and Cathaysia collided to form the South China Block. A large sedimentary basin forms on the previously thinned continental crust of the Yangtze Block.



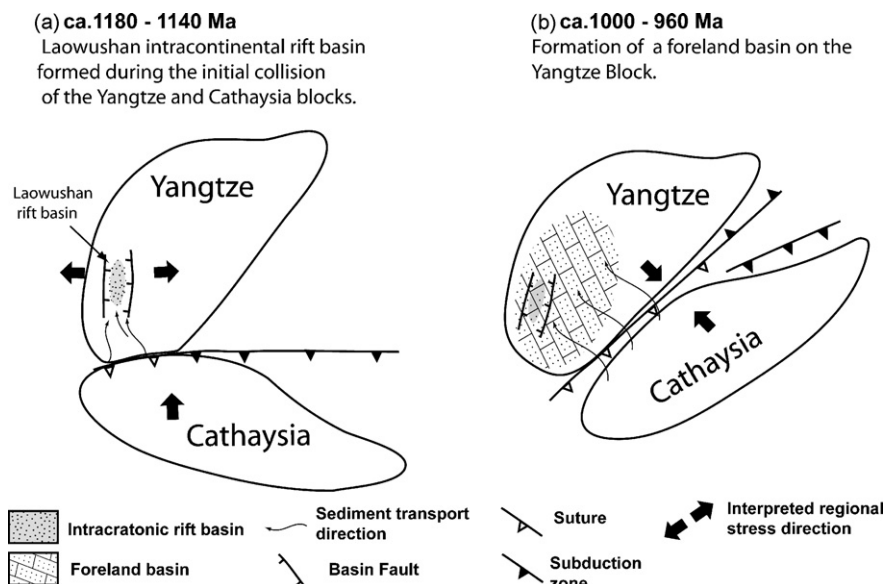


Fig. 17. Tectonic setting of late Mesoproterozoic–earliest Neoproterozoic basins in the western South China Block. (a) An inferred Laowushan rift basin orthogonal to an early collision between the Cathaysia and Yangtze Blocks. (b) The formation of a foreland basin on the Yangtze Block as a result of the collision of the Yangtze and Cathaysia Blocks during the Sibao Orogeny.

LREE pattern reflect the tholeiitic composition of the basalt. The HREE appear less fractionated than the other samples and have a  $(\text{Gd/Yb})_N = 1.8$ , suggesting the presence of garnet in the source. The tholeiitic composition of the basalts suggests they may have been erupted through a thinned continental crust in an area of high heat flow.

## 6.2. Tectonic implications

Our new SHRIMP data indicate late Mesoproterozoic to earliest Neoproterozoic ages for the sedimentary and volcanic rocks on the western margin of the Yangtze Block. These data show that the traditionally defined Kunyang Group can no longer be regarded as a single coherent sedimentary sequence, but rather as two distinct deposition sequences. The ages of the younger sequence overlaps with the late Mesoproterozoic to earliest Neoproterozoic Sibao Orogeny, reflecting the collision between the Yangtze and Cathaysia Blocks.

The Laowushan Formation defined in this study has a preliminary depositional age of  $1142 \pm 16$  Ma and contains alkali basalts with a geochemical and isotopic character similar to modern alkaline volcanic rocks from intracontinental rift settings such as the western branch of the East African Rift System or the central European volcanic province of the Rhine Graben. The Laowushan Formation is older than the ca. 1100 Ma intraplate magmatism found in Laurentia, Congo and Kalahari cratons that may have been spatially linked to a single large

igneous province during the Mesoproterozoic (Keller et al., 1989; Adams and Keller, 1994, 1996; Munyanyiwa, 1999; Dalziel et al., 2000; Ward et al., 2000; Hanson et al., 2004).

The Laowushan Formation contains ca. 1400 Ma detrital zircon grains. The only other rock from the Yangtze Block known to contain zircons of that age is the quartzite near Lala which Li et al. (2002b) interpreted as foreland basin deposits sourced from the Cathaysia Block (Fig. 15a and b). If such an interpretation also applies to the Laowushan Formation, it would suggest that the Yangtze and Cathaysia Blocks may have been partially joined as early as ca. 1140 Ma (Figs. 16a and b and 17a). However, this speculation requires that no 1400 Ma magmatic rocks exist on the Yangtze Block and they must represent sediment from an exotic derived terrain such as Cathaysia. To further understand the significance of the Laowushan Formation, the age span and geochemical characteristics of these rocks deserve further and more detailed investigation.

The clastic sediments of the Kunyang Group are consistent with being sourced from an uplifted orogenic belt to the present-day southeast and deposited in a foreland basin on the southern margin of the Yangtze Block, over an already thinned continental crust. The age spectrum of detrital grains suggests that early in the basins history sediments were dominantly derived from the late Archean and early Paleoproterozoic base-

ment rocks of the Yangtze Block (Figs. 9 and 15a), with a minor Mesoproterozoic ca. 1400 Ma component that has no known source on the Yangtze Block. Later in the basin history, sedimentation became more fluvial with increasing inputs from Paleoproterozoic to Mesoproterozoic (ca. 2000–1500 Ma) and late Mesoproterozoic to earliest Neoproterozoic (ca. 1275–960 Ma) terrains. The change in provenance may mark the uplifting of younger terrains along the Sibao orogenic belt. The foreland basin was active until at least 960 Ma. The absence of ca. 1400 Ma grains from the Liubatang Formation suggests that after ca. 960 Ma the Sibao orogenic belt had created a drainage divide which prevented Cathaysia-derived sediment from reaching the Yangtze side of the orogen.

Our work illustrates that if South China was indeed located in a central position in Rodinia (Li et al., 1995), the Kunyang Group may represent one of the rare basin records of Rodinia assembly during late Mesoproterozoic and earliest Neoproterozoic.

## Acknowledgments

This work was undertaken at the Tectonic Special Research Centre, The University of Western Australia, with a Chris Powell Memorial PhD Scholarship to MG. Fieldwork was supported by the TSRC, NSFC (Nos. 40032010B and 40421303), an ARC Discovery Project grant (No. DP0450020) and the Chinese Academy of Sciences project grant (No. 2003-2-1). The authors would like to thank Dr. W.X. Li and Mrs. Y. Liu for their assistance in the collection of ICP-MS and Nd isotope data at the Guangzhou Institute of Geochemistry at Guangzhou. Dr. N. Pearson, Dr. E. Belousova and Ms. S. Elhlou are thanked for their assistance with the acquisition and reduction of LA-ICPMS data at the GEMOC Key Centre, Macquarie University. All SHRIMP mounts were prepared at The University of Western Australia mineral separation laboratory with assistance from Mrs. Marian Marshall. The assistance of Dr. Bert de Waele with the setup and interpretation of SHRIMP data is gratefully acknowledged. Comments by Mark Barley and Peter Cawood significantly improved an earlier version of this manuscript. Gouchun Zhao and an anonymous reviewer are thanked for their careful and thorough reviews. Tectonic Special Research Centre publication #338 and a contribution to IGCP440.

## Appendix A. Supplementary data

Supplementary data associated with this article can be found, in the online version, at doi:10.1016/j.precamres.2006.08.002.

## References

- Adams, D.C., Keller, G.R., 1994. Possible extension of the Midcontinent Rift in west Texas and eastern New Mexico. *Can. J. Earth Sci.* 31, 709–720.
- Adams, D.C., Keller, G.R., 1996. Precambrian basement geology of the Permian Basin region of west Texas and eastern New Mexico: a geophysical perspective. *AAPG Bull.* 80, 410–431.
- Barrat, J.A., Fourcade, S., Jahn, B.M., Chemineé, J.L., Capdevila, R., 1998. Isotope (Sr, Nd, Pb, O) and trace-element geochemistry of volcanism from the Erta' Ale range (Ethiopia). *J. Volcanol. Geoth. Res.* 80, 85–100.
- Barrat, J.A., Jahn, B.M., Fourcade, S., Joron, J.L., 1993. Magma genesis in an ongoing rifting zone: the Tadjoura Gulf (Afar area). *Geochim. Cosmochim. Acta* 57, 2291–2302.
- Belousova, E.A., Griffin, W.L., Shee, S.R., Jackson, S.E., O'Reilly, S.Y., 2001. Two age populations of zircons from the Timber Creek kimberlites, Northern Territory, as determined by laser-ablation ICP-MS analysis. *Aust. J. Earth Sci.* 48, 757–765.
- Burchfiel, B.C., Wang, E., 2003. Northwest-trending, middle Cenozoic, left-lateral faults in southern Yunnan, China, and their tectonic significance. *J. Struct. Geol.* 25, 781–792.
- Chen, H., Ran, C., 1992. Isotope Geochemistry of Copper Deposits in Kangdian Axis. Geological Publishing House, p. 100 (Chinese with English abstract).
- Dalziel, I.W.D., Mosher, S., Gahagan, L.M., 2000. Laurentia–Kalahari collision and the assembly of Rodinia. *J. Geol.* 108, 499–513.
- Dewey, J.F., Windley, B.F. (Eds.), 1988. Palaeocene–Oligocene Tectonics of NW Europe. Early Tertiary Volcanism and the Opening of the NE Atlantic, vol. 39. Geological Society of London, London, pp. 25–31 (special publication).
- Frey, F.A., Green, D.H., Roy, S.D., 1978. Integrated models of petrogenesis: a study of quartz tholeiites to olivine melilitites from southeastern Australia utilizing geochemical and experimental petrologic data. *J. Petrol.* 19, 463–513.
- Hanson, R.E., Crowley, J.L., Bowring, S.A., Ramezani, J., Gose, W.A., Dalziel, I.W.D., Pancake, J.A., Seidel, E.K., Blenkinsop, T.G., Mukwakwami, J., 2004. Coeval large-scale magmatism in the Kalahari and Laurentian cratons during Rodinia assembly. *Science* 304, 1126–1129.
- Hao, J., Li, Y., Hu, Y., 1992. On the Jinning Movement and the Sianian System. *Reg. Geol. China* 2, 131–140 (Chinese with English abstract).
- Hu, A., Zhu, B., Mao, C.u., Zhu, N., Hunang, R., 1991. Geochronology of the Dahongshan Group. *Chin. J. Geochem.* 10 (3), 195–203.
- Huili, 1967. 1:200,000 geological map sheet. Sichuan Bureau of Geology and Mineral Resources.
- Humphris, S.E., Thompson, G.M., 1978. Hydrothermal alteration of oceanic basalts by seawater. *Geochim. Cosmochim. Acta* 42, 107–125.
- Jahn, B.M., Zhou, X.H., Li, J.L., 1990. Formation and tectonic evolution of South Eastern China and Taiwan: isotopic and geochemical constraints. *Tectonophysics* 183, 145–160.
- Keller, G.R., Hills, J.M., Baker, M.R., Wallin, E.T., 1989. Geophysical and geochronological constraints on the extent and age of mafic intrusions in the basement of west Texas and eastern New Mexico. *Geology* 17, 1049–1052.
- Kunming, 1971. 1:200,000 geological map sheet. Yunnan Bureau of Geology and Mineral Resources.
- Li, X.H., 1997. Timing of the Cathaysia Block formation: constraints from SHRIMP U–Pb zircon geochronology. *Episodes* 20 (3), 188–192.

- Li, X.H., Li, Z.X., Zhou, H., Liu, Y., Kinny, P.D., 2002a. U–Pb zircon geochronology, geochemistry and Nd isotopic study of Neoproterozoic bimodal volcanic rocks in the Kangdian Rift of South China: implications for the initial rifting of Rodinia. *Precamb. Res.* 113, 135–154.
- Li, Z.X., Li, X.H., Zhou, H., Kinny, P.D., 2002b. Grenvillian continental collision in South China: new SHRIMP U–Pb zircon results and implications for the configuration of Rodinia. *Geology* 30 (2), 163–166.
- Li, Z.X., Li, X.H., Kinny, P.D., Wang, J., Zhang, S., Zhou, H., 2003. Geochronology of Neoproterozoic syn-rift magmatism in the Yangtze Craton, South China and correlations with other continent: evidence for a mantle superplume that broke up Rodinia. *Precamb. Res.* 122, 85–109.
- Li, X.H., Liu, D., Sun, M., Li, W.X., Liang, X.R., Liu, Y., 2004. Precise Sm–Nd and U–Pb isotopic dating of the supergiant Shizhuyan polymetallic deposit and its host granite, SE China. *Geol. Mag.* 141 (2), 225–231.
- Li, Z.X., 1998. Tectonic history of the major East Asian lithospheric blocks since the Mid-Proterozoic-A synthesis. In: Martin, F.J., Chung, S.L., Lo, C.H., Lee, T.Y. (Eds.), *Mantle Dynamics and Plate Interactions in East Asia*. American Geophysical Union, Washington, DC, pp. 221–243.
- Li, Z.X., Powell, C.M., 2001. An outline of the palaeogeographic evolution of the Australasian region since the beginning of the Neoproterozoic. *Earth Sci. Rev.* 53 (3–4), 237–277.
- Li, Z.X., Zhang, L., Powell, C.M., 1995. South China in Rodinia: part of the missing link between Australia–East Antarctica and Laurentia? *Geology* 23, 407–410.
- Ludwig, K.R., 2001a. ISOPLOT/EX Version 2.49 A geochronological Toolkit for Microsoft Excel. Berkley Geochronological Centre Special Publication, No. 1a.
- Ludwig, K.R., 2001b. SQUID Version 1.02 A geochronological Toolkit for Microsoft Excel, Berkley Geochronological Centre Special Publication, No. 2.
- Ma, X.Y., Bai, J., 1998. *Precambrian Crustal Evolution of China*. Springer Verlag, Berlin, p. 331.
- Mattinson, J.M., Graubard, C.M., Parkinson, D.L., McClelland, W.C. (Eds.), U–Pb reverse discordance in zircons: the role of fine scale oscillatory zoning and sub-micron transport of Pb. *Earth Processes: Reading the Isotopic Code*, Geophysics Monograph 95. American Geophysical Union, pp. 355–370.
- McLaren, A.C., Fitzgerald, J.D., Williams, I.S., 1994. The microstructure of zircon and its influence on the age determination of from Pb/U isotopic ratios measured by ion microprobe. *Geochim. Cosmochim. Acta* 58, 993–1005.
- Moraes, R., Fuck, R.A., Pimentel, M.M., Costa Lima Gioia, S.M., Graciano Figueiredo, A.M., 2003. Geochemistry and Sm–Nd isotopic characteristics of bimodal volcanic rocks of Jucelândia, Goiás, Brazil: Mesoproterozoic transition from continental rift to oceanic basin. *Precamb. Res.* 125, 317–336.
- Munyanyiwa, H., 1999. Geochemical study of the Umkondo dolerites and lavas in the Chimanimani and Chipinge Districts (eastern Zimbabwe) and their regional implications. *J. Afr. Earth Sci.* 28 (2), 349–365.
- Norman, M.D., Pearson, N.J., Sharma, A., Griffin, W.L., 1996. Quantitative analysis of trace elements in geological materials by laser ablation ICPMS: instrumental operating conditions and calibration values of NIST glasses. *Geostandard. Newslett.* 20, 247–261.
- Pearce, J.A., 1975. Basalt geochemistry used to investigate past tectonic environments on Cyprus. *Tectonophysics* 25, 41–67.
- Pearce, J.A., 1983. Role of subduction lithosphere in magma genesis at active continental margins. In: Hawkesworth, C.J., Nory, M.J. (Eds.), *Continental Basalts and Mantle Xenoliths*. Shiva, Cheshire, UK, pp. 230–249.
- Pearce, J.A., Cann, J.R., 1971. Ophiolite Origin investigated by discriminate analysis using Ti, Zr and Y. *Earth Planet. Sci. Lett.* 12, 339–349.
- Pearce, J.A., Cann, J.R., 1973. Tectonic setting of basic volcanic rocks using determined using trace element analysis. *Earth Planet. Sci. Lett.* 19, 290–300.
- Pidgeon, R.T., Furfaro, D., Kennedy, A.K., Nemchin, A.A., Van Bronswijk, W., 1994. Calibration of zircon standards for the Curtin SHRIMP II, Abstracts of the 8th International Conference on Geochronology, Cosmochronology and Isotope Geology. US Geological Survey Circular, Berkley, USA, p. 251.
- Pik, R., Deneil, C., Coulon, C., Yirgu, G., Marty, B., 1999. Isotopic and trace element signatures of Ethiopian flood basalts: evidence for plume lithosphere interaction. *Geochim. Cosmochim. Acta* 63, 2263–2279.
- Qiu, Y.M., Gao, S., McNaughton, N.J., Groves, D.I., Ling, W., 2000. First Evidence of >3.2 Ga continental crust in the Yangtze Craton of South China and its implications for Archean Crustal Evolution and Phanerozoic Tectonics. *Geology* 28 (1), 11–14.
- Ran, C., 1983. Sedimentological environment and diagenetic metallogenesis of Dongchuan-type stratiform copper deposits in western Sichuan and Yunnan. *Geochemistry* 2 (4), 328–337 (English edition).
- Ran, C., 1989. Environmental significance of stromatolites and their relation to copper ore in the Louxue Formation of the Kunyang Group in Dongchuan, Yunnan, China. In: Boyle, W., Brown, C., Jefferson, W., Jowett, C., Kirkham (Eds.), *Sediment-Hosted Stratiform Copper Deposits*. Special Paper—Geological Association of Canada. Geological Association of Canada, Toronto, Canada, pp. 679–685.
- Ran, C., 1990. Geochemical data for the Dongchuan–Yimen strata-bound copper deposits, China. In: Parnell, J., Lianjun, Y., Changming, C. (Eds.), *Sediment-Hosted Mineral Deposits*. Special Publication of the International Association of Sedimentologists. Blackwell Scientific Publications, Beijing, Peoples Republic of China, pp. 173–180.
- Ritter, J.R.R., Jordan, M., Christensen, U.R., Achauer, U., 2001. A mantle plume below the Eifel volcanic fields, Germany. *Earth Planet. Sci. Lett.* 186, 7–14.
- Rogers, N., Macdonald, R., Fitton, J.G., George, R., Smith, M., Barreiro, B., 2000. Two mantle plumes beneath the East African rift system: Sr, Nd, and Pb isotope evidence from Kenya Rift basalts. *Earth Planet. Sci. Lett.* 176, 387–400.
- Ruan, H., Hua, R., Cox, D.P., 1991. Copper deposition by fluid mixing in deformed strata adjacent to a salt diapir, Dongchuan area, Yunnan province, China. *Econ. Geol.* 86, 1539–1545.
- Rubatto, D., Gebauer, D., 2000. Use of cathodoluminescence for U–Pb zircon dating by ion microprobe: some examples from the Western Alps. In: Pagel, M., Barbin, V., Blanc, P., Ohnenstetter, D. (Eds.), *Cathodoluminescence in Geosciences*. Springer Verlag, Berlin, p. 514.
- Sengor, A.M.C., Burke, K., Dewey, J.F., 1978. Rifts at high angles to orogenic belts: tests for their origin and the upper Rhine Graben as an example. *Am. J. Sci.* 278, 24–40.
- Shervias, J.W., 1982. Ti–V plots and the Petrogenesis of modern and Ophiolitic lavas. *Earth Planet. Sci. Lett.* 59, 101–118.
- Sircombe, K.N., 2003. AgeDisplay: an Excel workbook to evaluate and display univariate geochronological data using binned frequency

- histograms and probability density distributions. *Comput. Geosci.* 30, 21–31.
- Stacey, J.S., Kramers, J.D., 1975. Approximation of terrestrial lead isotope evolution by a two-stage model. *Earth Planet. Sci. Lett.* 26 (2), 207–221.
- Sun, S.S., McDonough, W.F. (eds.), 1989. Chemical and isotopic systematics of oceanic basalt: implications for mantle composition and processes. *Magmatism in the Ocean Basins*, vol. 42. Geological Society Special Publication.
- Thompson, R.N., Morrison, M.A., Henry, G.L., Parry, S.J., 1984. An assessment of the relative roles of crust and mantle in magma genesis: an elemental approach. *Philos. Trans. R. Soc. Lond., A* 310, 549–590.
- Ward, S.E., Hall, R.P., Hughes, D.J., 2000. Gurube and Mutare dykes: preliminary geochemical indication of complex Mesoproterozoic mafic magmatic systems in Zimbabwe. *J. Afr. Earth Sci.* 30 (3), 689–701.
- Wiedenbeck, M., 1995. An example of reverse discordance during ion microprobe zircon dating: an artefact of enhanced ion yields from a radiogenic labile Pb. *Chem. Geol.* 125, 197–218.
- Winchester, J.A., Floyd, P.A., 1977. Geochemical discrimination of different magma series and their differentiation products using immobile elements. *Chem. Geol.* 20, 325–343.
- Wood, D.A., 1980. The application of a Th–Hf–Ta diagram to problems of tectonomagmatic classification and to establishing the nature of crustal contamination of basaltic lavas of the British Tertiary volcanic province. *Earth Planet. Sci. Lett.* 50, 11–30.
- Wood, D.A., Joron, J.L., Treuil, M., 1979. A reappraisal of the use of trace elements to classify and discriminate between magma series erupted in different tectonic settings. *Earth Planet. Sci. Lett.* 45, 326–336.
- Wu, M., Duan, J., Song, X., Chen, L., 1990. Geology of the Kunyang Group in Yunnan Province. Yunnan Science and Technology Publishing House, Kunming, p. 265 (Chinese with English abstract).
- Xiong, X., Hou, S., Xue, S., 1995. Stratigraphy and the Deposit–Paleogeography of the Yinmin Formation of the Kunyang Group in Central Yunnan, vol. 3–5. China University of Geosciences Press, Wuhan, p. 96 (Chinese with English abstract).
- Yang, Z., Cheng, Y., Wang, H., 1986. The geology of China. In: *Oxford Monographs on Geology and Geophysics*, vol. 3. Oxford University Press, Oxford.
- Yongren, 1965. 1:200,000 scale geological map sheet. Sichuan Bureau of Geology and Mineral Resources.
- Yunnan, 1987. Regional Geology of Yunnan Province. People's Republic of China Ministry of Geology and Mineral Resources Geological Memoirs 1:500,000 Map and Explanatory Notes, vol. 21. Geological Publishing House, Beijing (Chinese with English summary).
- Yuxi, 1973. 1:200,000 geological map sheet. Yunnan Bureau of Geology and Mineral Resources.
- Zhang, Y., Wang, G., Jianfeng, N., Zhao, C., Xu, C., Qiu, J., Hao, W., 2003. Isotopic ages of the carbonatitic volcanic rocks in the Kunyang rift zone in central Yunnan, China. *Acta Geol. Sinica—Engl.* 77 (2), 204–211.
- Zhang, S.B., Zheng, Y.F., Wu, Y.B., Zhao, Z.F., Gao, S., Wu, F.Y., 2006. Zircon isotope evidence for >3.5 Ga continental crust in the Yangtze craton of China. *Precamb. Res.* 146, 16–34.
- Zhao, G., Cawood, P.A., 2000. Tectonothermal evolution of the Mayuan assemblage in the Cathaysia Block: implications for Neoproterozoic collision related assembly of the North and South China Craton. *Am. J. Sci.* 299, 309–339.
- Zhou, M., Yan, D., Kennedy, A.K., Li, Y., Ding, J., 2002a. SHRIMP U–Pb zircon geochronological and geochemical evidence for Neoproterozoic arc-magmatism along the western margin of the Yangtze Block, South China. *Earth Planet. Sci. Lett.* 196 (1–2), 51–67.